A Flea on Schrödinger's Cat

The Double Well Potential in the Classical Limit

Bachelor Thesis in Mathematics and Physics & Astronomy
Radboud Honours Academy Thesis

Robin Reuvers
Supervisor: Prof. dr. N.P. Landsman
Second reader: Dr. H. Maassen
August 2012
Radboud University Nijmegen

Preface

This thesis is the result of my bachelor project conducted during the third year of my bachelor degree program in Mathematics and in Physics & Astronomy at the Radboud University Nijmegen. It also serves as a thesis for my participation in the Radboud Honours Academy. The thesis discusses the double well potential in the classical limit, motivated by the idea that it might serve as a model for Schrödinger's Cat.

There are two versions of this thesis. The smaller one (in bit size) contains text and images like any other document. The larger one has a number of LaTeX beamer slides added to it at the end. These contain movies made in Matlab that demonstrate the numerical results presented in this thesis. They can be viewed with the standard Adobe viewer for pdf files, and perhaps with other programs as well. I will refer to these movies in both versions. A separate file that only contains the moving images is also available.

I would like to thank Klaas Landsman for the supervision of this project and for suggesting its direction. I very much appreciated your enthusiastic supervision, helpful comments and great advice during the past year. Of course, you also get the credit for coming up with the brilliant title of this thesis. Furthermore, I express my gratitude to Hans Maassen for being the second reader of this thesis and for answering questions about stochastic analysis. As to the Honours Academy, I am indebted to Wim van der Zande for his help during the past year. Finally, I want to thank Koen Reijnders and Timur Tudorovskiy for their ideas on how to approach the double well with WKB, and Willem Hundsdorfer for answering questions about numerical methods.

Contents

Chapter 1

Introduction

1.1 Schrödinger's Cat

Our motivation for studying the double well in the classical limit is the problem of *Schrödinger's Cat* in quantum mechanics. Therefore, we start with a description of Schrödinger's famous thought experiment [30]. The set-up is explained in Figure 1.1.

Figure 1.1: The set-up of the thought experiment known as Schrödinger's Cat. A cat is placed in a box. The box also contains a bottle of poison, a hammer, some radioactive material and a detector. Suppose we know that after a given time there is a fifty percent chance that at least one of the radioactive particles has decayed. Quantum mechanics admits this possibility because of the superposition principle. In case a particle decays, the detector notices this and causes a hammer to break the bottle of poison. This will kill the cat. When no particles decay, nothing happens and the cat continues to live. The particles are in a superposition of 'no particles decayed' and 'at least one particle decayed' (with equal probability), which apparently means that also the cat is in a superposition of 'alive' and 'dead'.[1]

Schrödinger's thought experiment brings a classical object (i.e. the cat) in a superposition. However, from experience we know that classical objects will never be in such a superposition. That means that something has to happen which causes the cat to make a choice to be either dead or alive.

[1] This image has been taken from the vast amount of pictures about Schödinger's Cat available on the Internet. Unfortunately, we could not recover its original source.

This is a special case of the *measurement problem* of quantum mechanics [3, 35]. This problem is concerned with the question what happens when a measurement is performed. Up to this date, no satisfying answer to this question has been found.

1.2 The classical limit

Quantum mechanics is a theory that provides an accurate description of systems containing tiny particles, but in principle it can be applied to any physical system. As we known from centuries of experience, classical physics works just fine for large and familiar objects. We therefore expect that if we apply quantum mechanics to such objects, it reproduces classical results. This is what we call the *classical limit*. Here are two examples in which such a classical limit is important.

Example 1.2.1. Consider the Schrödinger equation for a single free particle:

$$i\hbar\frac{d\psi}{dt} = -\frac{\hbar^2}{2m}\frac{d^2\psi}{dx^2} \equiv H\psi,$$

If we apply this equation to a particle with large mass, the Schrödinger equation should reproduce classical mechanics. But what do we mean by a large mass? To make clear what this means, we should introduce a typical energy scale ϵ and a typical length scale λ. We then rescale the Hamiltonian as H/ϵ and write it in terms of the dimensionless variable $\tilde{x} = x/\lambda$ to see that

$$\frac{H}{\epsilon} = -\frac{\hbar^2}{2m\epsilon\lambda^2}\frac{d^2}{d\tilde{x}^2} \equiv -\tilde{\hbar}^2\frac{d^2}{d\tilde{x}^2}, \tag{1.1}$$

where we have introduced the dimensionless quantity $\tilde{\hbar} = \frac{\hbar}{\lambda\sqrt{2m\epsilon}}$. In this way, large mass effectively means small $\hbar$.

Example 1.2.2. Now consider Planck's law:

$$\frac{E_\nu}{N_\nu} = \frac{h\nu}{e^{h\nu/k_BT} - 1}$$

This equation produces classical behaviour when $h\nu << k_BT$, which is either the limit of high temperature or of small frequency. This means that the dimensionless quantity $\frac{h\nu}{k_BT} \to 0$.

In both the above examples, the classical limit corresponds to the limit where a certain dimensionless quantity becomes small. In the first example, this is caused by a large mass, but in the second, it is due to a high temperature. In both cases, however, it can also be achieved by letting $\hbar \to 0$ at fixed m and T, respectively. At first this seems ridiculous, for $\hbar$ is a physical constant. How can it change its value? Indeed, it cannot, but as a mathematical trick, letting $\hbar \to 0$ can be very useful to model the classical limit. It turns out that for many systems the classical limit can be linked to the limit $\hbar \to 0$ in this way, which makes the trick broadly applicable. In this thesis, we will often make use of it and refer to the classical limit as $\hbar \to 0$. When we do this, the meaning of the limit $\hbar \to 0$ can always be translated to a genuine physical limit that is well understood. Sometimes, we will also refer to the classical limit in a different way, depending on the situation at hand. More about the classical limit can be found in [21].

1.3 A problem similar to Schrödinger's Cat

Now that we have linked the classical limit to the artificial limit $\hbar \to 0$, it is time to look at the situation we will study in this thesis: the *double well potential*. This potential is widely used in physics and has been studied extensively [6, 14, 20]. In this thesis, we look at it in a very unusual way, i.e. as a model for Schrödinger's Cat. How can this possibly be done? Before we answer that question, we first look at the double well in a bit more detail.

A typical double well potential is depicted in Figure 1.2. Needless to say, it consists of two wells separated by a barrier. When a particle obeying *classical mechanics* has an energy below the height of the barrier, its motion is restricted to one of the wells. We can also say that the two wells are decoupled. The ground state is doubly degenerate: the particle can be at either the left or the right minimum.

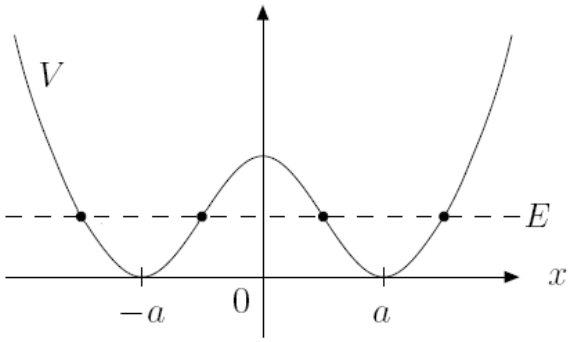

Figure 1.2: A double well potential. Classically, tunneling is not allowed, so the particle is in one of the wells. Consequently, the ground state is doubly degenerate.

Quantum mechanics tells a different story since it allows the particle to tunnel through the barrier. This lifts the degeneracy of the ground state and causes a small energy splitting to appear between the ground state and first excited state. Figure 1.3 shows the ground state and first excited state of a particle in a double well.

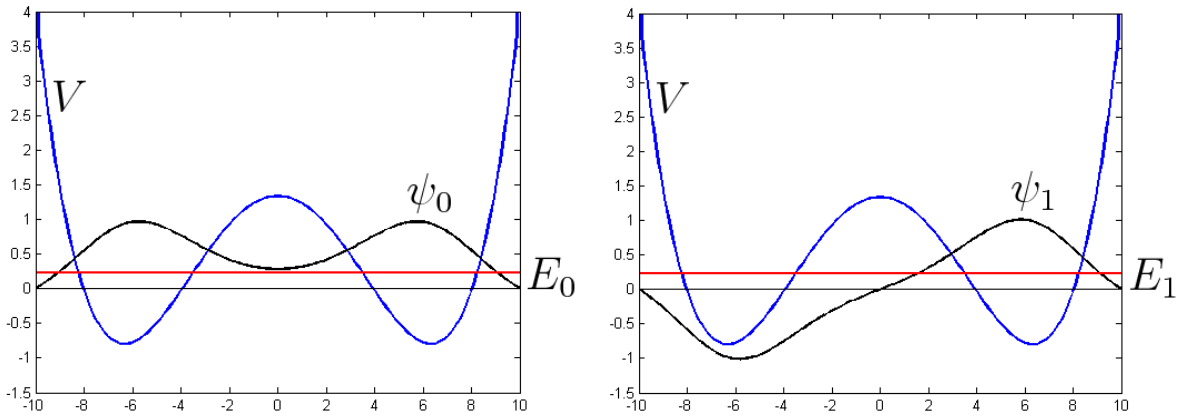

(a) Ground state.

(b) First excited state.

Figure 1.3: A double well potential with its ground state and first excited state. A particle in either of these states can be found in both wells due to tunneling. We will later introduce the term 'delocalized' to describe this kind of behaviour.

We will now see what happens when we take the classical limit by letting $\hbar \to 0$. Figure 1.4 shows the ground state of the double well for different $\hbar$. We see that the wave function centers around the minima as $\hbar \to 0$. In fact, this pattern continues and we end up with two infinitely narrow peaks around the minima. This can be seen very well in the added movie *Classical limit 1*. This kind of behaviour is not what we expect to see in the classical limit. Instead, the wave function should move to either the left or the right well, since we know that a classical particle can only be in one well at the same time. What we find, however, is a superposition of the classical states 'left' and 'right'. It is in this sense that the problem is comparable to that of Schrödinger's Cat, which also concerns a superposition of classical states. We can therefore hope that a solution to the problem of the double well potential leads to a better understanding, and possibly a solution, of the problem of Schrödinger's Cat.

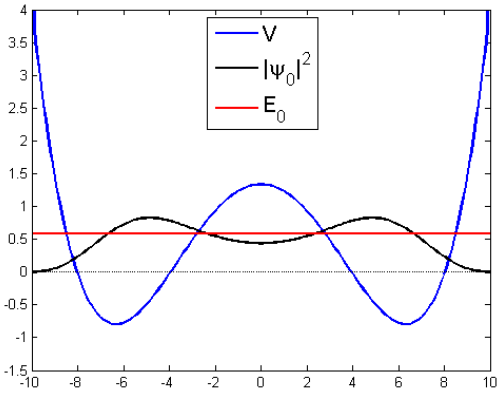

(a) The ground state for $\hbar_a$.

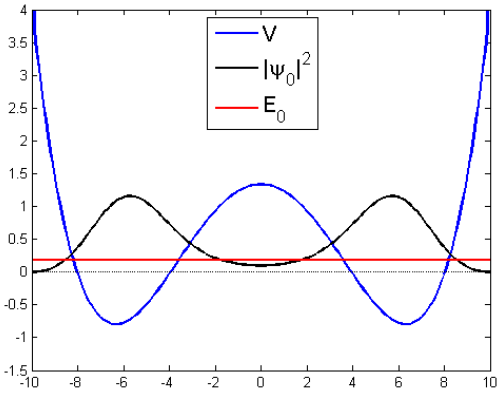

(b) The ground state for $\hbar_b$.

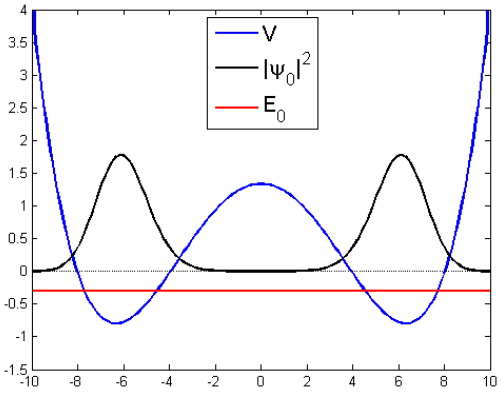

(c) The ground state for $\hbar_c$.

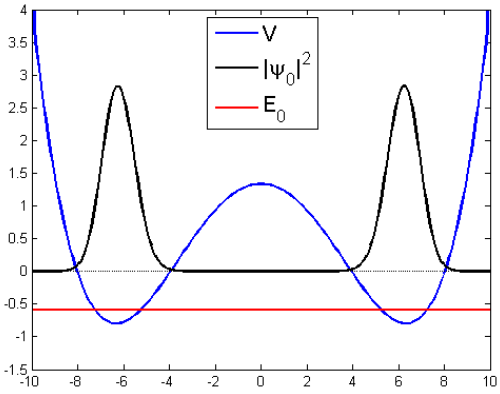

(d) The ground state for $\hbar_d$.

Figure 1.4: These images show the ground state of an unperturbed double well potential for different $\hbar$. In fact, $\hbar_a > \hbar_b > \hbar_c > \hbar_d$. As $\hbar$ becomes smaller, the peaks center around the minima and get narrower.

1.4 A solution?

For this new problem, it appears there might be a solution available in the literature. It is based on a phenomenon called 'the flea on the elephant', first discussed in [16, 17]. The idea is the following: we introduce a small perturbation in the right well, as can be seen in Figure 1.5. Once again we check how the ground state behaves as $\hbar \to 0$. Figure 1.5 shows what happens: the ground state wave function moves entirely to the left well! This means that the classical limit no longer leads to a superposition of classical states, which solves our problem. The effect is also demonstrated by the added movie *Classical limit 2*. The new ground state can be described as *localized*, as opposed to the *delocalized* one in Figure 1.3. The process of moving from a delocalized state to a localized one, is what we call *localization* of the wave function. Note that time does not play any role in the process: we simply display the ground state of the potential for different $\hbar$. We therefore call this effect *time-independent localization*. It can be distinguished from *time-dependent localization*, which is the localization of a certain initial wave function due to the time evolution of the system as dictated by the Hamiltonian.

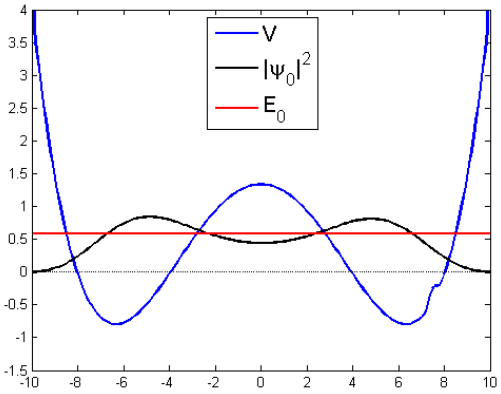

(a) The ground state for $\hbar_a$.

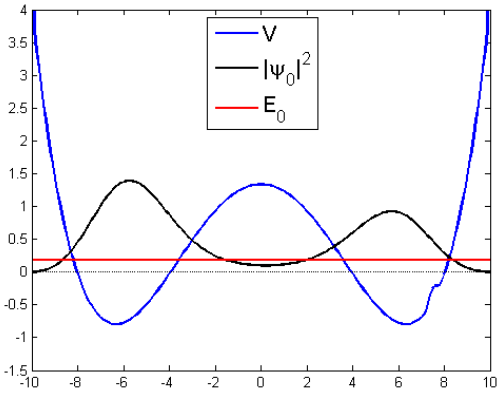

(b) The ground state for $\hbar_b$.

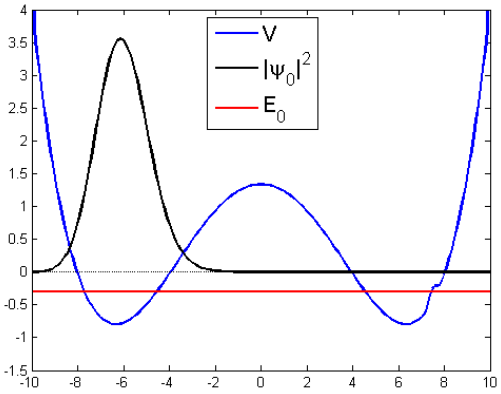

(c) The ground state for $\hbar_c$.

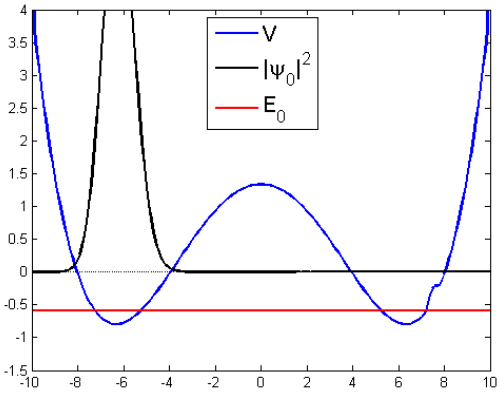

(d) The ground state for $\hbar_d$.

Figure 1.5: These images show the ground state of a perturbed double well potential for different $\hbar$. In fact, $\hbar_a > \hbar_b > \hbar_c > \hbar_d$. For $\hbar_a$ there is barely any difference with the ground state of an unperturbed double well potential (the first image of Figure 1.4). However, as $\hbar$ becomes smaller, the wave function moves entirely to the left well. We say that the ground state has localized in a time-independent way.

But is this really a solution to our problem? The answer is: no, unfortunately. In the context of the measurement problem, the classical limit $\hbar \to 0$ does not stand on its own. A measurement can only be realized by letting $t \to \infty$ as well, i.e. time evolution is present. Therefore, the localization we need has to be time-dependent. Our candidate solution has so far offered us time-independent localization,

which by itself is unsatisfactory. There is an upside to this disappointing conclusion: it provides us with a great topic for further research. We could ask the question: does this time-independent localization have a time-dependent analogue? And so: can small perturbations indeed force the system to leave its superposition and make a choice between the classical states? Or, adopting the view of a novelist: can a small flea, tightly lodged in the fur of Schrödinger's Cat, pass final judgement on his host?

1.5 The aim of this project

To answer the questions posed above, both the time-independent and time-dependent behaviour of the double well must be studied. The aim of this project therefore is twofold.

On the one hand we want to find out more about the time-independent behaviour of the double well potential in the classical limit. To do this, we first reduce the double well to a two-level system, for which we can easily do calculations. What little we can say about the time-independent aspects of this simplified system is contained in Chapter 2. We then turn to the real, more complicated system: the double well potential. In Chapter 3, we approach it in two ways that are very different in character: the first is the traditional WKB approximation from physics, and the second is the mathematical field of semiclassical analysis. The former contains approximations, but is quite intuitive and makes calculations easy. The results of the latter have a certainty that physicists can only dream of, but sometimes it is hard to see what is actually going on. We will try to combine these two methods and compare their results, getting a good overview of the time-independent aspects of the problem. This finishes the first part of the thesis.

On the other hand we want to look at the time-dependent behaviour of the double well. Our main question in this part of the thesis is: does the time-independent localization due to a perturbation discussed in Section 1.4 have a time-dependent analogue? We start looking for an answer by studying a perturbed two-level system in a time-dependent way in Chapter 4. To make things realistic, we also add stochastic perturbations that can model noise caused by a classical environment. Using stochastic calculus, we can get an idea of the average behaviour of the two-level system, i.e., the average taken over multiple double wells with different noises. This is not enough however, since we would like to be able to predict the outcome of a single experiment, so that we can be certain of the occurrence of localization. That is why we will also use numerical methods to simulate such experiments. Of course, we will compare the results of these two approaches. It is then time to look at the double well potential in a time-dependent way in Chapter 5. This is the system we are most interested in, but it is also the most complicated system we will study. We will therefore have to limit ourselves to using numerical methods to obtain results. Nonetheless, enough can be said.

At the end of this thesis, we summarize our conclusions and relate them to the problem of Schrödinger's Cat. That way, we will get closer to finding out whether small perturbations can cause the cat to make a choice and be dead or alive.

Part I

Time-Independent Results

Chapter 2

Two-Level System

Before we look at the double well, we discuss a simplified version of it. When we assume that the lowest two energy levels of a double well are far away from the rest, at low energy, it can be seen as a two-level system. The two level system is also important for the double well in the classical limit, as can be seen from the use of a so-called interaction matrix in [11, 32]. It even has a very clear modern application: the qubits of quantum computers are two-level systems. In the time-independent case there is not much to study about the two-level system, which is the reason for the limited length of this chapter. Things will become more interesting in Chapter 4.

To study this system we define the two basis vectors as the 'left' and 'right' states:

$$\psi_L = \begin{pmatrix} 1 \\ 0 \end{pmatrix}, \qquad \psi_R = \begin{pmatrix} 0 \\ 1 \end{pmatrix}. \tag{2.1}$$

We regard these states as 'localized'. We define the unperturbed Hamiltonian of the system:

$$H = \begin{pmatrix} 0 & -\epsilon \\ -\epsilon & 0 \end{pmatrix}, \tag{2.2}$$

where ϵ is a positive constant. The two eigenstates of H are:

$$\psi_0 = \frac{1}{\sqrt{2}} \begin{pmatrix} 1 \\ 1 \end{pmatrix} = \psi_L + \psi_R \quad \text{with energy} \quad E_0 = -\epsilon \ , \tag{2.3}$$

$$\psi_1 = \frac{1}{\sqrt{2}} \begin{pmatrix} 1 \\ -1 \end{pmatrix} = \psi_L - \psi_R \quad \text{with energy} \quad E_1 = \epsilon \ . \tag{2.4}$$

That means we are dealing with a ground state and a first excited state which are 'delocalized' and are separated by an energy splitting 2ϵ. This is also the case for a double well, which is where the analogy comes in. We conclude that 2ϵ should be seen as the energy splitting between the lowest two energy levels. We will discuss various approximations for this splitting in Section 3.3. In this respect, the reader should keep in mind that $\epsilon \to 0$ as $\hbar \to 0$, as we will see later.

We now add a perturbation ΔV to the Hamiltonian:

$$H' = \begin{pmatrix} \Delta V & -\epsilon \\ -\epsilon & 0 \end{pmatrix}. \tag{2.5}$$

Note that H and H' have the same effect on ψ_R. However, they treat ψ_L differently. That is why we say the perturbation has been added 'on the left'.

The eigenvalues of H' are:

$$E_0' = \frac{\Delta V}{2} - \frac{1}{2}\sqrt{\Delta V^2 + 4\epsilon^2}, \tag{2.6}$$

$$E_1' = \frac{\Delta V}{2} + \frac{1}{2}\sqrt{\Delta V^2 + 4\epsilon^2}, \tag{2.7}$$

with normalized eigenvectors

$$\psi_0' = \left(\frac{\Delta V^2}{2} + 2\epsilon^2 + \frac{\Delta V}{2}\sqrt{\Delta V^2 + 4\epsilon^2}\right)^{-1/2} \begin{pmatrix} \epsilon \\ \frac{\Delta V}{2} + \frac{1}{2}\sqrt{\Delta V^2 + 4\epsilon^2} \end{pmatrix}, \tag{2.8}$$

$$\psi_1' = \left(\frac{\Delta V^2}{2} + 2\epsilon^2 - \frac{\Delta V}{2}\sqrt{\Delta V^2 + 4\epsilon^2}\right)^{-1/2} \begin{pmatrix} \epsilon \\ \frac{\Delta V}{2} - \frac{1}{2}\sqrt{\Delta V^2 + 4\epsilon^2} \end{pmatrix}. \tag{2.9}$$

We are interested in the classical limit $\hbar \to 0$. It is good to note that this limit is equivalent to the limit $\frac{\Delta V}{\epsilon} \to \infty$, which can also be caused by very strong noise. For $\Delta V > 0$, this leads to

$$\psi_0' = \begin{pmatrix} 0 \\ 1 \end{pmatrix} = \psi_R \quad \text{with energy} \quad E_0' = 0 \ , \tag{2.10}$$

$$\psi_1' = \begin{pmatrix} 1 \\ 0 \end{pmatrix} = \psi_L \quad \text{with energy} \quad E_1' = \Delta V \ . \tag{2.11}$$

This means that the ground state moves to the unperturbed 'right' and the first excited state moves to the perturbed 'left'. However, for $\Delta V < 0$, we find the opposite result

$$\psi_0' = \begin{pmatrix} 1 \\ 0 \end{pmatrix} = \psi_L \quad \text{with energy} \quad E_0' = \Delta V \ , \tag{2.12}$$

$$\psi_1' = \begin{pmatrix} 0 \\ -1 \end{pmatrix} = -\psi_R \quad \text{with energy} \quad E_1' = 0 \ . \tag{2.13}$$

In this case, the ground state moves to the perturbed 'left' and the first excited state moves to the unperturbed 'right'. When we put ΔV in the right well (i.e. it is on the lower position in the diagonal of the Hamiltonian), the eigenvectors switch place and so do the above conclusions.

We conclude that for each nonzero perturbation ΔV, the ground state and first excited state localize as $\hbar \to 0$ (which implies that $\epsilon \to 0$). That is, there is time-independent localization in the classical limit. In the next chapter, we will see that the above results resemble the behaviour of the double well in the classical limit.

Chapter 3

Double Well Potential

In this section we look at the time-independent aspects of the double well. We study and compare two methods that are very different in character. The first is the (physical) WKB method discussed in Section 3.1. It contains approximations, but makes numerous calculations easy. The second is the (mathematical) field of semiclassical analysis discussed in Section 3.2. The use of mathematics makes its results certain, but its scope is restricted to the actual limit $\hbar \to 0$, and sometimes it is hard to see what is really going on. It is interesting to see what these methods can tell us about the double well. Will they give comparable results, and will those results be in agreement with numerical simulations? We discuss this in the final section of this chapter.

What are we going to study with these methods anyway? First of all, we are interested in so-called *energy splittings*. These are certain differences between energy levels that appear in a double well because of the coupling between the individual wells. We should make that a bit more precise. In a slightly naive view, one could see the double well as a pair of decoupled harmonic oscillators. In this case the ground state is degenerate. In fact, this is approximately the right way of looking at the problem when the barrier is relatively high and broad, i.e. the classical limit. Outside this limit, however, the particle can tunnel trough the barrier in the middle. This lifts the degeneracy and introduces a first excited state ψ_1 with a slightly higher energy than the ground state ψ_0. The difference in energy $E_1 - E_0$ is known as the *ground state energy splitting*. Higher energy levels are also paired in this way (e.g. E_2 is far from E_1 but close to E_3) and the energy splittings between these pairs are known as *higher state energy splittings* (e.g. $E_3 - E_2$). It turns out it is good to know how these energy splittings depend on $\hbar$. For example, the two-level system defined in Chapter 2 contains the ground state energy splitting of the double well. After this, we turn to the actual wave function. The most important question will be: what do these two methods tell us about time-independent localization of the wave function when perturbations are present? We will see that both methods predict this localization, and that the results will be in accordance with numerical simulations.

3.1 Double well with WKB

The WKB method is widely used in physics as a semiclassical approximation technique. Here, we apply it to the double well potential. A review of the WKB approximation in general can be found in Appendix A. The most important results of the appendix are the WKB wave functions (A.15),(A.16) and the connection matrices (A.42), (A.43).
The method used in Section 3.1.1 and Section 3.1.2 comes from [1] and is accurate for higher state energy splittings. The one used in Section 3.1.4 is based on [7] and is a correction of this result for the ground state energy splitting. This method relies on the derivation of Herring's formula in Section 3.1.3, which comes from [20]. In fact, [20] also contains a derivation of the energy splittings, but it leads to the same result as [1].

3.1.1 Energy levels in a single well

Consider the potential well in Figure 3.1. We start out by deriving a quantization condition for the energy levels of such a well. It serves as a nice example for things to come. Figure 3.1 also introduces the notation we will use.

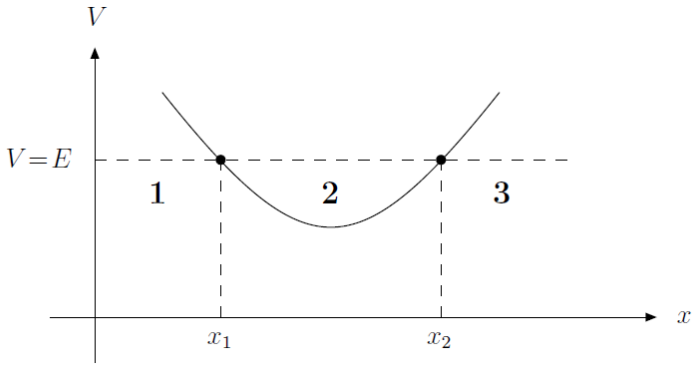

Figure 3.1: A general potential well V. The particle has energy E. This provides us with turning points x_1 and x_2 and regions 1, 2 and 3. This picture has been taken from [1]

We connect the WKB wave function in area 1 (with coefficients C_l and D_l) to the WKB wave function in area 3 (with coefficients C_r and D_r). Before we start, we look how the coefficients A_l, B_l, A_r and B_r are related. Of course, they should describe the same wave function, therefore

$$\begin{aligned} &A_l e^{\frac{i}{\hbar}\int_{x_1}^{x} p(x)dx} + B_l e^{-\frac{i}{\hbar}\int_{x_1}^{x} p(x)dx} \equiv \\ &A_r e^{\frac{i}{\hbar}\int_{x_2}^{x} p(x)dx} + B_r e^{-\frac{i}{\hbar}\int_{x_2}^{x} p(x)dx} = \\ &\quad A_r e^{-\frac{i}{\hbar}\int_{x_1}^{x_2} p(x)dx} e^{\frac{i}{\hbar}\int_{x_1}^{x} p(x)dx} + B_r e^{\frac{i}{\hbar}\int_{x_1}^{x_2} p(x)dx} e^{-\frac{i}{\hbar}\int_{x_1}^{x} p(x)dx}. \end{aligned} \tag{3.1}$$

We now use the following notation

$$\theta = \frac{1}{\hbar}\int_{x_1}^{x_2} p(x)dx, \tag{3.2}$$

so that the transition can be described as

$$\begin{pmatrix} A_l \\ B_l \end{pmatrix} = \overbrace{\begin{pmatrix} e^{-i\theta} & 0 \\ 0 & e^{i\theta} \end{pmatrix}}^{M_{A_r/B_r \to A_l/B_l}} \begin{pmatrix} A_r \\ B_r \end{pmatrix}. \tag{3.3}$$

We are now ready to connect the wave functions in areas 1 and 3. First note that $\psi(x) \to 0$ as $x \to \infty$ because otherwise the wave function will not be square-integrable. Starting in area 3, we see that $D_r = 0$.

Using the connection matrices in (A.42) and (A.43), we see that

$$\begin{pmatrix} C_l \\ D_l \end{pmatrix} = \overbrace{e^{-i\pi/4}\begin{pmatrix} 1 & i \\ \frac{i}{2} & \frac{1}{2} \end{pmatrix}}^{M_{A_l/B_l \to C_l/D_l}} \overbrace{\begin{pmatrix} e^{-i\theta} & 0 \\ 0 & e^{i\theta} \end{pmatrix}}^{M_{A_r/B_r \to A_l/B_l}} \overbrace{e^{i\pi/4}\begin{pmatrix} 1 & -\frac{i}{2} \\ -i & \frac{1}{2} \end{pmatrix}}^{M_{C_r/D_r \to A_r/B_r}} \begin{pmatrix} C_r \\ 0 \end{pmatrix},$$

which leads to

$$\begin{pmatrix} C_l \\ D_l \end{pmatrix} = C_r \begin{pmatrix} 2\cos\theta \\ \sin\theta \end{pmatrix}. \tag{3.4}$$

Of course, we also demand that $\psi(x) \to 0$ as $x \to -\infty$. Therefore, $C_l = 2\cos(\theta) = 0$. This leads to a quantization condition for the allowed energies:

$$\boxed{\int_{x_1}^{x_2} p(x)dx = \int_{x_1}^{x_2} \sqrt{2m\,[E - V(x)]}dx = (n + \frac{1}{2})\pi\hbar \quad (n = 0, 1, 2, \ldots)\,.} \tag{3.5}$$

We can also conclude that

$$C_r = (-1)^n D_l. \tag{3.6}$$

Finally, the WKB wave function is

$$\begin{aligned} \psi^{\text{WKB}}_{\text{area 1}}(x) &= \tfrac{D_l}{\sqrt{|p(x)|}} e^{-\frac{1}{\hbar}\int_x^{x_1}|p(x)|dx}; \\ \psi^{\text{WKB}}_{\text{area 2}}(x) &= \tfrac{2D_l}{\sqrt{p(x)}} \cos\left[\tfrac{1}{\hbar}\int_{x_1}^{x} p(x)dx - \tfrac{\pi}{4}\right] = \tfrac{2C_r}{\sqrt{p(x)}} \cos\left[\tfrac{1}{\hbar}\int_{x}^{x_2} p(x)dx - \tfrac{\pi}{4}\right]; \\ \psi^{\text{WKB}}_{\text{area 3}}(x) &= \tfrac{C_r}{\sqrt{|p(x)|}} e^{-\frac{1}{\hbar}\int_{x_2}^{x}|p(x)|dx}. \end{aligned} \tag{3.7}$$

A final remark should be made: this approximation is only accurate for higher energy levels, as explained in [1].

3.1.2 Higher state energy splitting in the symmetric double well

Now consider a symmetric double well, as shown in Figure 3.2. We will use a method from [1] to calculate the energy splittings for this well. Once again, the figure introduces the notation used.

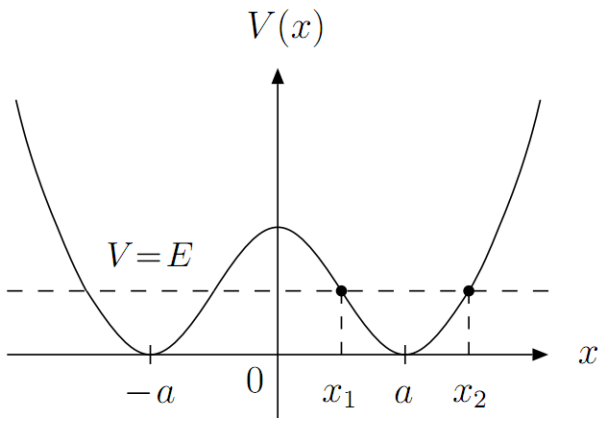

Figure 3.2: A symmetric double well potential V. The minima are $-a$ and a. We assume that the particle has energy E. This provides us with turning points x_1, $-x_1$, x_2 and $-x_2$. This figure is a modified version of a figure in [1].

We use results obtained in Appendix A to find the approximate energy levels below the barrier ($E < V(0)$). Using (3.4) and (A.16), the wave function for $-x_1 < x < x_1$ can be written as:

$$\psi^{\text{WKB}}_{(-x_1,x_1)}(x) = \frac{1}{\sqrt{|p(x)|}} \left(2C_r\cos(\theta)e^{\frac{1}{\hbar}\int_x^{x_1}|p(x)|dx} + C_r\sin(\theta)\, e^{-\frac{1}{\hbar}\int_x^{x_1}|p(x)|dx}\right), \tag{3.8}$$

where C_r is the coefficient of the WKB solution in the interval (x_2, ∞).
Since the potential is even, we know there exist energy eigenfunctions that are even (ψ_+^{WKB}) or odd (ψ_-^{WKB}). For these wave functions, we know that:

$$\frac{d}{dx}\psi_+^{\mathrm{WKB}}\bigg|_{x=0} = 0 \qquad \text{and} \qquad \psi_-^{\mathrm{WKB}}(0) = 0 \ . \tag{3.9}$$

When we apply these conditions to (3.8), we find

$$\sin(\theta)e^{-\frac{1}{\hbar}\int_0^{x_1}|p(x)|dx} = \pm 2\cos(\theta)e^{\frac{1}{\hbar}\int_0^{x_1}|p(x)|dx}, \tag{3.10}$$

making use of the fact that V, and therefore p, is even, which means that $p'(0) = 0$. The symbol $\pm$ depends on the corresponding wave function. From this, we conclude that

$$e^{-\frac{1}{\hbar}\int_{-x_1}^{x_1}|p(x)|dx} = \frac{\pm 2}{\tan(\theta)}, \tag{3.11}$$

where we again use the fact that p is even to change the boundary of the integral.

Now suppose the barrier $(-x_1, x_1)$ is very high and broad. Then we can assume the term on the left side of the previous equation to be negligible. This leads to the familiar quantization condition (3.5). This makes sense: tunneling through a very high and broad barrier is almost impossible, which means that the particle is localized in one of the wells. Then, the allowed energies are of course the same as those of the single potential well we discussed before. In this case, it does not matter whether the wave function is even or odd. Both have the corresponding energy level of the single potential well, which we shall denote by $E_n^{(0)} (n = 0, 1, \ldots)$.

For a high and broad barrier, it is therefore reasonable to write

$$\boxed{E_{n,\pm}^{\mathrm{WKB}} = E_n^{(0)} + \Delta E_{n,\pm} \qquad (n = 0, 1, \ldots) \ ,} \tag{3.12}$$

where $\Delta E_{n,\pm}$ is much smaller than $E_n^{(0)}$. In this case, the following equations holds approximately:

$$\theta(E_{n,\pm}^{\mathrm{WKB}}) \approx (n + \frac{1}{2})\pi + \theta'(E_n^{(0)})\Delta E_{n,\pm}, \tag{3.13}$$

$$\int_{-x_1}^{x_1}\sqrt{2m\left[V(x) - E_{n,\pm}^{\mathrm{WKB}}\right]}dx \approx \int_{-x_1}^{x_1}\sqrt{2m\left[V(x) - E_n^{(0)}\right]}dx. \tag{3.14}$$

From this and (3.11) we conclude that

$$\Delta E_{n,\pm} \approx \mp\frac{1}{2\theta'(E_n^{(0)})}\exp\left[-\frac{1}{\hbar}\int_{-x_1}^{x_1}\sqrt{2m\left(V(x) - E_n^{(0)}\right)}dx\right], \tag{3.15}$$

where we have used the identity $\tan(n\pi + \frac{\pi}{2} + x) = -1/x$.
This implies that each energy level of the single potential well is split into two energy levels of a double potential well. The lower of the two corresponds to an even wave function (since $\Delta E_{n,\pm}$ is positive), the higher to an odd wave function. We can also see that the splitting becomes large if the energy increases or the barrier decreases in height and width, since the integral in the last expression decreases in that case. As we have seen, the energy splitting dissappears for a very high and broad barrier.
Equation (3.15) can be put into a slightly different form by writing

$$\begin{aligned}
\theta'(E_n^{(0)}) &= \frac{d}{dE}\left[\frac{1}{\hbar}\int_{x_1}^{x_2}\sqrt{2m\left(E_n^{(0)} - V(x)\right)}dx\right] \\
&= \frac{1}{\hbar}\int_{x_1}^{x_2} m^{1/2}\left[2\left(E_n^{(0)} - V(x)\right)\right]^{-1/2}dx \\
&= \frac{1}{\hbar}\int_{x_1}^{x_2}\frac{1}{v_n(x)}dx = \frac{T_n}{2\hbar},
\end{aligned} \tag{3.16}$$

where $v_n(x)$ is the speed of a classical particle with energy $E_n^{(0)}$ at position x, and T_n is the time a classical particle with energy $E_n^{(0)}$ takes to move from x_1 to x_2 and back. Using the fact that $\omega = 2\pi/T$, we conclude

$$\boxed{\Delta E_{n,\pm} \approx \mp \frac{\omega_n \hbar}{2\pi} \exp\left[-\frac{1}{\hbar}\int_{-x_1}^{x_1} \sqrt{2m\left(V(x) - E_n^{(0)}\right)}dx\right].} \tag{3.17}$$

Note that this derivation is based on the work done in Section 3.1.1. The approximation derived there, however, was only accurate for higher energy levels (i.e. higher n). This means that (3.17) does not predict the ground state energy as accurately as possible. It turns out that the constant in front of the exponential should change a bit. We derive this correction in the next section.

3.1.3 Herring's formula

Although the previous derivation is not accurate enough for the ground state, (3.12) remains true: for each energy level of the single potential well $E_n^{(0)}$ there exists a symmetric ($\psi_{n,+}$) and an antisymmetric ($\psi_{n,-}$) eigenstate of the double well, which has approximately the same energy. Let $\psi_n^{(0)}$ be the wave function of a particle in the right well with energy $E_n^{(0)}$, normalized so that $\int_0^\infty |\psi_n^{(0)}(x)|^2 dx = 1$. In this subsection, we are going to calculate a general expression for the energy splitting in terms of $\psi_n^{(0)}$.
We now assume that $\psi_{n,+}$ and $\psi_{n,-}$ can be approximated by $\psi_n^{(0)}$ in the following way:

$$\psi_{n,\pm}(x) = \frac{1}{\sqrt{2}}\left[\psi_n^{(0)}(x) \pm \psi_n^{(0)}(-x)\right]. \tag{3.18}$$

Of course, $\psi_n^{(0)}$ and $\psi_{n,\pm}$ obey the Schrödinger equation:

$$\psi_{n,\pm}''(x) + \frac{2m}{\hbar^2}\left[E_{n,\pm} - V(x)\right]\psi_{n,\pm}(x) = 0\ , \tag{3.19}$$

$$\psi_n^{(0)\prime\prime}(x) + \frac{2m}{\hbar^2}\left[E_n^{(0)} - V(x)\right]\psi_n^{(0)}(x) = 0\ . \tag{3.20}$$

When we subtract the above equations, and integrate the result over $(0,\infty)$, we find

$$E_{n,\pm} - E_n^{(0)} = \frac{\hbar^2}{2m}\left[\int_0^\infty \psi_n^{(0)\prime\prime}\psi_{n,\pm} - \psi_n^{(0)}\psi_{n,\pm}''dx\right]\left[\int_0^\infty \psi_n^{(0)}\psi_{n,\pm}dx\right]^{-1}. \tag{3.21}$$

We use the fact that $\psi_{n,+}(0) = \sqrt{2}\psi_n^{(0)}(0)$ and $\psi_{n,+}'(0) = 0$ and similar expressions for $\psi_{n,-}$ to conclude that

$$\int_0^\infty \psi_n^{(0)\prime\prime}\psi_{n,\pm} - \psi_n^{(0)}\psi_{n,\pm}''dx = \mp\sqrt{2}\psi_n^{(0)}(0)\psi_n^{(0)\prime}(0). \tag{3.22}$$

By assuming that $\psi_n^{(0)}(-x)$ is negligible for $x \in (0,\infty)$, we see that

$$\int_0^\infty \psi_n^{(0)}\psi_{n,\pm}dx \cong \frac{1}{\sqrt{2}}\int_0^\infty |\psi_n^{(0)}|^2 = \frac{1}{\sqrt{2}}. \tag{3.23}$$

Combining all this, we find

$$\boxed{E_{n,\pm} - E_n^{(0)} = \Delta E_{n,\pm} = \mp\frac{\hbar^2}{m}\psi_n^{(0)}(0)\psi_n^{(0)\prime}(0)\ ,} \tag{3.24}$$

which is know as Herring's formula. It is named after Herring, who derived it in the analysis of a problem relating the H_2^+ molecular ion [12, 13].

3.1.4 Corrected ground state energy splitting of a symmetric double well

In this subsection, we use Herring's formula to find an expression for the energy splitting of the ground state: $\Delta E_{0,\pm}$. We suppose $\psi_0^{(0)}$ to equal its WKB wave function in the classically forbidden region $(-x_1, x_1)$:

$$\psi_0^{(0)}(x) \approx \frac{C}{\sqrt{|p(x)|}} e^{\frac{1}{\hbar}\int_0^x |p(x')|dx'}, \tag{3.25}$$

where we have set $D = 0$ in the WKB wave function (A.16), since $\psi_0^{(0)}$ is the wave function of a particle located in the right well. We calculate:

$$\psi_0^{(0)'}(x) \approx \left(\frac{|p(x)|}{\hbar} - \left| \frac{p'(x)}{2p(x)} \right| \right) \psi_0^{(0)}(x) \approx \frac{|p(x)|}{\hbar} \psi_0^{(0)}(x), \tag{3.26}$$

where we neglect the second term since the system is in a semiclassical state by assumption.
Together with (3.24) and (3.25), this leads to

$$\Delta E_{0,\pm} = \mp \frac{\hbar}{m} C^2. \tag{3.27}$$

We have already assumed that $\psi_0^{(0)}$ can be approximated by its WKB wave function in the classically forbidden region $(-x_1, x_1)$. It is time for a second assumption: the potential $V(x)$ can be approximated in (x_1, x_2) by a harmonic oscillator potential which has its minimum at $x = a$:

$$V(x) \approx \frac{1}{2} m\omega_0 (x-a)^2, \tag{3.28}$$

where ω_0 is the same as in (3.17). This means both the ground state energy and wave function and resemble those of the harmonic oscillator:

$$E_0^{(0)} \approx \frac{1}{2}\hbar\omega_0, \tag{3.29}$$

$$\psi_0^{(0)}(x) \approx \left(\frac{m\omega_0}{\pi\hbar}\right)^{1/4} \exp\left[-\frac{m\omega_0}{2\hbar}(x-a)^2\right]. \tag{3.30}$$

We assume that this approximation of the wave function remains valid in the region $(-x_1, x_1)$. Therefore, we can determine C by comparing (3.25) and (3.30). To do this, we calculate $|p(x)|$ in the region $(-x_1, x_1)$:

$$\begin{aligned} |p(x)| &= \sqrt{2m\left[V(x) - E_0^{(0)}\right]} \\ &= \sqrt{2m\left[V(x) - V(x_1)\right]} \\ &= m\omega_0 \left[(a-x)^2 - (a-x_1)^2\right]^{1/2}. \end{aligned} \tag{3.31}$$

Note that we can approximate $x_1 - a$ by using (3.29):

$$u_0 \equiv a - x_1 \approx \left(\frac{\hbar}{m\omega_0}\right)^{1/4}. \tag{3.32}$$

The term u_0^2 may be neglected in evaluating $|p(x)|^{1/2}$ in (3.25) since $a - x > a - x_1$ for $x \in (-x_1, x_1)$, and the barrier is rather broad. This implies

$$\psi_0^{(0)}(x) \cong \frac{C}{\sqrt{m\omega_0(a-x)}} \exp\left[\frac{1}{\hbar}\int_0^{x_1} |p(x)|dx + \Phi(x)\right], \tag{3.33}$$

where

$$\begin{aligned} \Phi(x) &= -\frac{1}{\hbar}\int_x^{x_1} |p(x')|dx' \\ &= -\frac{m\omega_0}{\hbar}\int_x^{x_1} \left[(a-x')^2 - (a-x_1)^2\right]^{1/2} dx' \\ &\approx -\frac{m\omega_0(a-x)^2}{2\hbar} + \frac{1}{2}\ln\left(\frac{2(a-x)}{u_0}\right) + \frac{1}{4} + O\left(\frac{u_0^2}{(a-x)^2}\right), \end{aligned} \tag{3.34}$$

which we find from a Taylor expansion. By comparing the previous equation with (3.30), we find

$$C = \left(\frac{m^2\omega^2}{4\pi e}\right)^{1/4} \exp\left[-\frac{1}{\hbar}\int_0^{x_1} |p(x)|dx\right]. \tag{3.35}$$

Plugging this into (3.27), we obtain

$$\begin{aligned}\Delta E_{0,\pm} &= \mp\frac{\hbar\omega_0}{2\sqrt{\pi e}} \exp\left[-\frac{1}{\hbar}\int_{-x_1}^{x_1} |p(x)|dx\right] \\ &= \mp\frac{\hbar\omega_0}{2\sqrt{\pi e}} \exp\left[-\frac{1}{\hbar}\int_{-x_1}^{x_1} \sqrt{2m\left(V(x) - E_0^{(0)}\right)}dx\right].\end{aligned} \tag{3.36}$$

This expression is an important result, since it provides a more accurate ground state energy splitting of the double well than the one derived in Section 3.1.2. Note that it only differs from (3.17) (the 'wrong' approximation) by a factor $(\pi/e)^{1/2} \approx 1,075$.
This procedure can also be applied for higher energy levels. All one needs to do is match the WKB wave function in the classically forbidden region $(-x_1, x_1)$ to the nth harmonic oscillator state and use Herring's formula to find $\Delta E_{n,\pm}$. As can be read in [7], the correction factor approaches 1 for higher n as we would expect.

3.1.5 A quantization condition for an asymmetric double well

We would like to use the WKB method to say something about an asymmetric double well. To do this, we cannot use the method in Section 3.1.2, because we have used the fact that the potential was symmetric there. Actually, the ideas from Section 3.1.4 can be used, as discussed in [33]. Here, we look at a different method, which aims to use connection formulas similar to the approach presented in Section 3.1.1. At first glance, it seems we can apply the method used there, i.e. we start on the left and by repeatedly using the connection formulas (A.42) and (A.43) we move to the right. That way, we would obtain two equations which would lead to a quantization condition. However, these connection formulas have a one-directional nature, i.e. they can only be used one way. That means they are in fact incorrect! This delicate situation is explained in [6, 29]. Most common textbooks on quantum mechanics state and use these connection formulas anyway and for simple potentials like a single well they produce correct results. This is no longer the case for a more complicated potential like the double well. Thus, we really need to beware of the limited applicability of the connection formulas. We will not study this one-directional nature of connection formulas in this thesis, but we simply state a correct method for tackling the asymmetric double well, using a result from [29].

Consider a general asymmetric well, as shown in Figure 3.3. This figure introduces part of the notation used.

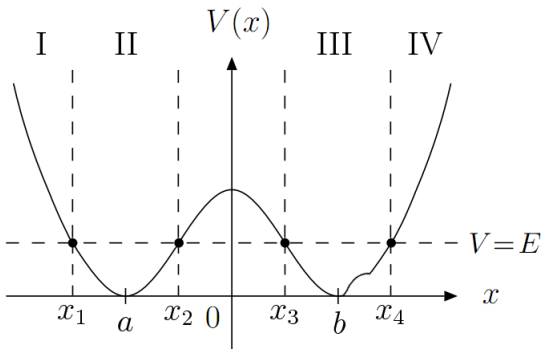

Figure 3.3: An asymmetric double well potential V. The minima are a and b. We assume that the particle has energy E. This provides us with turning points x_1, x_2, x_3 and x_4 and five regions. Four of these regions are named with Roman numerals. This figure is a modified version of a figure in [1].

We need some more notation for the WKB coefficients used in our calculation. As in (A.15) and (A.16), A, B and C, D denote the coefficients of the WKB wave function in the classically allowed region and the classically forbidden region, respectively. The number attached to a letter shows to which turning point it belongs, e.g. A_1 and B_1 are the coefficients of the WKB wave function in region II with respect to x_1 (i.e. x_1 is the lower boundary of the integral in (A.15)). It turns out we also need the following three quantities:

$$\theta_1 = \frac{1}{\hbar}\int_{x_1}^{x_2} p(x)dx, \qquad \theta_2 = \frac{1}{\hbar}\int_{x_3}^{x_4} p(x)dx, \qquad K = \frac{1}{\hbar}\int_{x_2}^{x_3} |p(x)|dx. \tag{3.37}$$

We are interested in the limit $K \to \infty$, since this implies that the barrier is very high and broad, which corresponds to the classical limit $\hbar \to 0$. A final quantity we need is

$$\tilde{\phi} = \arg\left[\Gamma\left(\frac{1}{2} + i\frac{K}{\pi}\right)\right] + \frac{K}{\pi} - \frac{K}{\pi}\ln\left(\frac{K}{\pi}\right). \tag{3.38}$$

The reader can check that $\tilde{\phi} \to 0$ as $K \to \infty$.

Our goal is the following quantization condition for the general double well in Figure 3.3:

$$\boxed{\left(1 + e^{-2K}\right)^{1/2} = \frac{\cos(\theta_1 - \theta_2)}{\cos(\theta_1 + \theta_2 - \pi + \tilde{\phi})}\,.} \tag{3.39}$$

This condition can be found in the following way:

1. We start out in region I (coefficients C_1 and D_1). As before, we immediately see that $C_1 = 0$, for the wave function needs to be square-integrable.

2. Using the left connection matrix from (A.42), we move to region II (coefficients A_1 and B_1). We can then use the reasoning in (3.1) and (3.3) to write the WKB wave function with respect to x_2. The result is
$$\begin{pmatrix} A_2 \\ B_2 \end{pmatrix} = e^{i\pi/4}\begin{pmatrix} -ie^{i\theta_1} \\ e^{-i\theta_1} \end{pmatrix} D_1. \tag{3.40}$$

3. In a similar way, we start in region IV (coefficients C_4 and D_4) and see that $D_4 = 0$. After moving to III with a connection matrix and rewriting the wave function with respect to x_3, we find
$$\begin{pmatrix} A_3 \\ B_3 \end{pmatrix} = e^{i\pi/4}\begin{pmatrix} e^{-i\theta_2} \\ -ie^{i\theta_2} \end{pmatrix} C_4\,. \tag{3.41}$$

4. We now use a result from [29] to jump over the barrier and connect the WKB wave functions in region II and III:
$$\begin{pmatrix} A_2 \\ B_2 \end{pmatrix} = \begin{pmatrix} \left(1 + e^{2K}\right)^{1/2} e^{-i\tilde{\phi}} & ie^{K} \\ -ie^{K} & \left(1 + e^{2K}\right)^{1/2} e^{i\tilde{\phi}} \end{pmatrix}\begin{pmatrix} A_3 \\ B_3 \end{pmatrix}. \tag{3.42}$$

5. Combining the above results (i.e. inserting (3.40) and (3.41) in (3.42)), we find two equations:
$$\frac{D_1}{C_4} = i\left[\left(1 + e^{2K}\right)^{1/2} e^{-i(\theta_1+\theta_2+\tilde{\phi})} + e^{K}e^{-i(\theta_1-\theta_2)}\right], \tag{3.43}$$
$$\frac{D_1}{C_4} = -i\left[\left(1 + e^{2K}\right)^{1/2} e^{i(\theta_1+\theta_2+\tilde{\phi})} + e^{K}e^{i(\theta_1-\theta_2)}\right]. \tag{3.44}$$

6. The equality of the above two equations leads to the quantization condition (3.39).

With this quantization condition and (3.43), we can say something about energy levels and the wave function in an asymmetric double well. This will be discussed in the next few sections.

3.1.6 Energy splitting in an asymmetric double well potential

Assume that for a certain (unperturbed) symmetric double well and given energy E, the constants θ_1 and θ_2 equal θ. As in Figure 3.3, we introduce a perturbation in the right well. For example, by (3.38), this means that $\theta = \theta_1 > \theta_2$ for a positive perturbation. We therefore write $\theta_1 = \theta$, $\theta_2 = \theta - \delta$ with $\delta \in \mathbb{R}$ (e.g. $\delta > 0$ in Figure 3.3). The quantization condition (3.39) then becomes

$$\left(1 + e^{-2K}\right)^{1/2} = \frac{\cos(\delta)}{\cos(2\theta - \delta - \pi + \tilde{\phi})} \ . \tag{3.45}$$

We can solve for θ:

$$\boxed{\theta = (n + \frac{1}{2})\pi + \frac{1}{2}\delta - \frac{1}{2}\tilde{\phi} \mp \frac{1}{2} \arccos\left[\frac{\cos(\delta)}{\left(1 + e^{-2K}\right)^{1/2}}\right].} \tag{3.46}$$

This resembles the original quantization condition (3.5) for a single well. Here, the energy levels have split up in pairs around the original ones (where the sign $-$ in the equation corresponds to the lower energy by (3.38)). To get a good idea of what this means, we will examine this equation for two special cases.

We first set $\delta = 0$ and check if this reproduces the results we have seen before for the symmetric double well:

$$\theta = (n + \frac{1}{2})\pi - \frac{1}{2}\tilde{\phi} \mp \frac{1}{2} \arccos\left[\frac{1}{\left(1 + e^{-2K}\right)^{1/2}}\right]. \tag{3.47}$$

Supposing that K is large, that means that

$$\theta \approx (n + \frac{1}{2})\pi \mp \frac{1}{2}e^{-K}, \tag{3.48}$$

since for K large, $\tilde{\phi} \approx 0$ and $\arccos\left(\frac{1}{\sqrt{1+x^2}}\right) = \arctan x \approx x$ for small x. We once again find that the energy levels of the single well have split in two. One can check with a technique similar to the one used in (3.12)-(3.16) that this result leads exactly to (3.17). So, our method for a general double well leads to the results found previously for a symmetric double well. Now that this has been confirmed, let us look at (3.46) in the classical limit $K \to \infty$.

Solving (3.46) for $K \to \infty$ (and so $\tilde{\phi} \to 0$) gives

$$\theta = \begin{cases} (n + \frac{1}{2})\pi & \text{for } - \text{ in (3.46) (lower energy)} \\ \delta + (n + \frac{1}{2})\pi & \text{for } + \text{ in (3.46) (higher energy)} \end{cases} \ . \tag{3.49}$$

This is different from the symmetric well, which gives a twofold degeneracy for each energy level labeled by n in the limit $K \to \infty$. Equation (3.49) can be understood in the following way: in the classical limit, tunneling is suppressed. Therefore, the particle is localized in one of the wells, where it obeys the quantization condition (3.5) for a single well. If it is in the left well, then $\theta_1 = (n + \frac{1}{2})\pi = \theta$, but if it is in the right well, we have $\theta_2 = (n + \frac{1}{2})\pi = \theta - \delta$.

3.1.7 Localization in an asymmetric double well potential

Now that we have analyzed the behaviour of the energy splitting, we turn to the WKB wave function. With the notation used in the previous section, (3.43) leads to

$$\frac{D_1}{C_4} = i\left[\left(1 + e^{2K}\right)^{1/2} e^{-i(2\theta - \delta + \tilde{\phi})} + e^{K} e^{-i\delta}\right]. \tag{3.50}$$

By inserting (3.46) and doing some calculations, the reader can check that for $\delta \in [-\pi, \pi]$ one has

$$\boxed{\frac{D_1}{C_4} = \sin(\delta)e^{K} \pm \sqrt{\sin^2(\delta)e^{2K} + 1} \ .} \tag{3.51}$$

This allows us to say something about localization of the WKB wave function in the classical limit $K \to \infty$. As can be seen from (3.40), D_1 is a measure of the amplitude of the WKB wave function in regions I and II in Figure 3.3. In a similar way, (3.41) shows that C_4 is a measure of the amplitude of the WKB wave function in regions III and IV. Therefore, the fraction D_1/C_4 gives an indication of whether and where the wave function is localized. Doing the same calculation again for $\delta \in [\pi, 3\pi]$ gives the above result multiplied by -1. Of course, this can be generalized: for $n \in \mathbb{Z}$ and $\delta \in [(2n-1)\pi, (2n+1)\pi]$, the result (3.51) is correct for n even and should be multiplied by -1 for n odd. This will not have much effect on our conclusions, as we will see.
We consider some cases and check what (3.51) tells us:

- For $\delta = 0$ (no perturbation), we find that $\frac{D_1}{C_4} = \pm 1$.
  Remember that the general double well has pairs of energy levels (labeled by n). Such a pair consists of a lower and higher lying level, corresponding to $-$ and $+$ in (3.46), respectively. Here, we see that for the lower level $D_1 = C_4$, i.e. the WKB wave function is even. However, for the higher level $D_1 = -C_4$, which means the WKB wave function is odd. Of course, we already knew this and we have even used it in Section 3.1.2 to derive the energy splitting in a symmetric double well. Nonetheless, it is nice to see our new method produces this result. Also note that this is not only independent of n, but also of K, which is what we would expect.

- For $\delta > 0, \delta \notin \{k\pi | k \in \mathbb{Z}\}$ (a positive perturbation in the right well, e.g. the potential in Figure 3.3), we find in the limit $K \to \infty$ that:

$$\frac{D_1}{C_4} \longrightarrow \begin{cases} \infty & \text{for } - \text{ in (3.46) (lower energy)} \\ 0 & \text{for } + \text{ in (3.46) (higher energy)} \end{cases} .$$

  For the lower (higher) energy, the WKB wave function is localized on the left (right).

- For $\delta < 0,\ \delta \notin \{k\pi | k \in \mathbb{Z}\}$ (a negative perturbation in the right well), we find that:

$$\frac{D_1}{C_4} \longrightarrow \begin{cases} 0 & \text{for } - \text{ in (3.46) (lower energy)} \\ \infty & \text{for } + \text{ in (3.46) (higher energy)} \end{cases} .$$

  For the lower (higher) energy, the WKB wave function is localized on the right (left).

- For $\delta \in \{k\pi | k \in \mathbb{Z}\backslash\{0\}\}$, something strange happens and we find either $\frac{D_1}{C_4} = \pm 1$ or $\frac{D_1}{C_4} = \mp 1$. This implies that no localization takes place, which is unexpected. It can probably be explained by level crossing, i.e. certain energy levels of the two individual wells coincide.

- All this time we have interpreted δ as the result of a perturbation in the right well. However, a review of our approach shows that it allows us to interpret a positive perturbation in the right well as a negative one in the left well and vice versa. Therefore, the above results change place if we put the perturbation in the left well.

Our method produces the results we would expect. However, something is not quite right about the above reasoning. We have treated δ as a constant, but in reality it depends on K. The reason for this is that K affects θ_1 and θ_2, and therefore $\delta = \theta_1 - \theta_2$, via the quantization condition. We can ask whether the above results are correct. To answer this question, consider a fixed energy level (i.e. fixed n and $\pm$ in (3.46)) in a given double well potential that has a perturbation in one of the wells. In the limit of completely decoupled wells ($K \to \infty$), we know this energy level has some fixed limit higher than the minimum of the potential. As long as the perturbation is below this energy level, we know that $\theta_1 - \theta_2 \neq 0$ by (3.38). This means there exists some K_0 such that $|\theta_1 - \theta_2| \neq 0$ for any $K > K_0$. We can then apply the above reasoning to see our conclusions about localization are still correct. To make things easier, we have ignored the 'special' case $\delta \in \{k\pi | k \in \mathbb{Z}\backslash\{0\}\}$ here.

In Section 3.3 we will compare these results to the ones obtained by the rigorous mathematical treatment of the problem. For now, we remark that the conclusions are in complete agreement with the numerical time-independent results, which already have been presented in Section 1.3 and Section 1.4.

3.2 Flea on the Elephant

In this section, we approach the matters discussed in the previous one from a new point of view. That is the field of semiclassical analysis, which is definitely mathematical in character. The name of this section refers to the most important theorem we will discuss. The term *flea on the elephant* was first used by Simon in [32] to describe a phenomenon found by Jona-Lasinio, Martinelli and Scoppola [16, 17] in the theory of one-dimensional Schrödinger operators. It has also been discussed by others [10, 11]. In this section we discuss a number of results by Simon [31, 32] about this phenomenon in arbitrary dimensions. We will then check what this means for the double well in one dimension. The reader interested in this particular case, can skip to Section 3.2.3 right away.

3.2.1 Preliminaries

For a given potential $V(x)$ defined on $\mathbb{R}^\nu$, the corresponding *Schrödinger operator* on the Hilbert space $L^2(\mathbb{R}^\nu)$ is defined as

$$H(\hbar) = -\hbar^2\Delta + V(x), \tag{3.52}$$

where we write H as a function of $\hbar$, since we are interested in the limit $\hbar \to 0$. This is an unbounded operator, which complicates matters. Nonetheless, its behaviour is well understood [14, 28], and we will not look into it any further. Note that this is the operator that appears in the Schrödinger equation with mass $m = \frac{1}{2}$. Let $\lambda = 1/\hbar$. We can rewrite this operator as

$$H(\hbar) = H(1/\lambda) = -\frac{1}{\lambda^2}\Delta + V(x) = \frac{1}{\lambda^2}(-\Delta + \lambda^2 V(x)). \tag{3.53}$$

We define

$$H^S(\lambda) = -\Delta + \lambda^2 V(x), \tag{3.54}$$

noting that the behaviour of H as $\hbar \to 0$ is closely linked to the behaviour of H^S as $\lambda \to \infty$. It is exactly this Hamiltonian that is studied in [31, 32], together with the Schrödinger equation

$$i\frac{\partial \psi}{\partial t} = H^S(\lambda)\psi, \tag{3.55}$$

which might seem unusual to physicists because a factor $\hbar$ is missing on the left compared to the usual Schrödinger equation. This is important to consider when we want to compare the results discussed in this section to the WKB results (which we will do later on).

We now make some assumptions about V. Let V be a function on $\mathbb{R}^\nu$ satisfying

1. V is C^∞ and non-negative;
2. V is strictly positive at ∞, i.e. $V(x) \geq \delta$ if $|x| > R$ for some $R,\ \delta > 0$;
3. $V(Ax) = V(x)$ for some Euclidian transformation A of order 2. In one dimension, this would mean the potential has to be even;
4. V is zero at exactly two points m_1 and m_2, where $Am_1 = m_2$;
5. $\partial^2 V/\partial x_i \partial x_j(m_1)$ is a non-singular matrix. As a consequence, $\partial^2 V/\partial x_i \partial x_j(m_2)$ is non-singular as well.

Now we define a suitable (pseudo)metric.

Definition 3.2.1. Given a function V on $\mathbb{R}^\nu$ that satisfies conditions $1-5$ above, we define the *Agmon metric* ρ_V by

$$\rho_V(x,y) = \inf\left\{ \int_0^1 \sqrt{V(\gamma(s))}\ |\dot\gamma(s)|ds \;\middle|\; \gamma \text{ continuous}, \gamma(0) = x, \gamma(1) = y \right\}, \tag{3.56}$$

for $x, y \in \mathbb{R}^\nu$. This metric is independent of λ.

Note that under these conditions, the Agmon distance is the geodesic distance in the Riemann metric $V(x)dx^2$.
The main result of [31] is:

Theorem 3.2.2. *Let $V(x)$ be a function satisfying conditions $1-5$ above. Let $H^S(\lambda)$ and ρ_V be defined as above. Let $E_0^S(\lambda)$ and $E_1^S(\lambda)$ be the two lowest eigenvalues of $H^S(\lambda)$. Then*

$$\lim_{\lambda\to\infty} -\lambda^{-1}\ln\left[E_1^S(\lambda)-E_0^S(\lambda)\right]=\rho_V(m_1,m_2). \tag{3.57}$$

In fact, this theorem can be proved with fewer assumptions, as pointed out in [14, 31].

Remark 3.2.3. Consider the one-dimensional case ($\nu=1$). Note that the geodesic with respect to the Agmon metric connecting any two points x and y is a straight line from x to y. So, we know that

$$\rho_V(x,y)=\left|\int_x^y\sqrt{V(s)}ds\right|. \tag{3.58}$$

This resembles the term used in the WKB method for a particle with energy 0 and mass $1/2$. By using (3.53) and (3.55), we see that the two lowest eigenenergies of $H(\hbar)$ with respect to the usual Schrödinger equation are $E_0(\hbar)=\hbar E_0^S(\lambda)$ and $E_1(\hbar)=\hbar E_1^S(\lambda)$. This allows us to write the conclusion of Theorem 3.2.2 in terms of $\hbar$:

$$\lim_{\hbar\to 0}\ -\hbar\ \ln\left[\frac{E_1(\hbar)-E_0(\hbar)}{\hbar}\right]=\rho_V(m_1,m_2). \tag{3.59}$$

For $\hbar$ sufficiently small, this means that [1]

$$E_1(\hbar)-E_0(\hbar)\approx\hbar\exp\left[-\frac{1}{\hbar}\left|\int_{m_1}^{m_2}(V(s))^{1/2}ds\right|\right]. \tag{3.60}$$

Later on, we will compare this expression to the results obtained in Section 3.1.

We are also interested in the eigenfunctions of $H^S(\lambda)$. The following is known rigorously from [31]:

Theorem 3.2.4. *Let $V(x)$ be a function satisfying conditions $1-5$ above. Let $H^S(\lambda)$ and ρ_V be defined as above. Denote by $\psi_n(x,\lambda)$ the $(n+1)$th eigenfunction of $H^S(\lambda)$. Then, for any $x\in\mathbb{R}^\nu$,*

$$\limsup_{\lambda\to\infty}\ \lambda^{-1}\ln|\psi_n(x,\lambda)|\ \leq\ -\min\{\rho_V(x,m_1),\rho_V(x,m_2)\}. \tag{3.61}$$

Since $\rho_V(x,y)>0$ if $x\neq y$, one sees that this theorem implies that $\psi_n(x,\lambda)\to 0$ as $\lambda\to\infty$ if $x\notin\{m_1,m_2\}$.

We need one more definition.

Definition 3.2.5. The *vacuum limiting set* $A(\psi_0)$ is defined by:

$$x\in A(\psi_0)\qquad\Longleftrightarrow\qquad\forall\ \text{neighbourhood } N \text{ of } x:\ \lim_{\lambda\to\infty}\ \frac{1}{\lambda}\ \ln\left(\|\chi_N\psi_0\|\right)=0, \tag{3.62}$$

where χ_N is the characteristic function of N. By Theorem 3.2.4, this means that $A(\psi_0)\subset\{m_1,m_2\}$.

This definition allows us to say something about the *localization* of the wave function. If a point is contained in $A(\psi_0)$, it means that ψ_0 wil not go to zero at that point as $\lambda\to\infty$. Therefore, if only one of m_1,m_2 is contained in the vacuum limiting set, we see that the ground state is localized (at that point). In an unperturbed double well potential that satisfies the properties $1-5$ above, the ground state is delocalized (and so $A(\psi_0)=\{m_1,m_2\}$). This can be proved relatively easily given an additional property of the potential.

[1] The precise meaning of this approximation is $(E_1(\hbar)-E_0(\hbar))\exp\left[\frac{1}{\hbar}\left|\int_{m_1}^{m_2}(V(s))^{1/2}ds\right|\right]=\mathcal{O}(\hbar)$. This will also be the case later on, when we state similar approximations.

Proposition 3.2.6. *Let ψ_0 be the ground state of the Schrödinger operator with V as above. We then know that $\psi_0(Ax) = \psi_0(x)$. Suppose $\lim_{|x|\to\infty} V(x) = \infty$. This implies that $V(\psi_0) = \{m_1, m_2\}$, which means the ground state is delocalized.*

Proof. It is easy to check that $\psi_0^A(x) \equiv \psi_0(Ax)$ is also a solution of the Schrödinger equation with the same eigenvalue and norm. In Appendix B, we state Theorem B.2.4 and check that the potential V satisfies its conditions. We then know that the ground state ψ_0 of V is nondegenerate. Therefore, $\psi_0 = \psi_0^A$, which implies $\psi_0(x) = \psi_0(Ax)$. That means that $V(\psi_0)$ has to contain both m_1 and m_2, or nothing at all. The latter is impossible, since that would contradict the normalization of the eigenstate. Therefore, $V(\psi_0) = \{m_1, m_2\}$. □

3.2.2 Adding a perturbation

We now add a term W to the potential, which is a function on $\mathbb{R}^\nu$ satisfying

1. W is C^∞ and non-negative;
2. W is bounded;
3. $W(x) \equiv 0$ for x near m_1 or m_2.

It turns out that the addition of W may have a dramatic effect on the ground state wave function for $\hbar \to 0$. When we think of W as a flea and of the wave function as an elephant, following [32], this means that the flea causes the elephant to shift its weight. That is where the name of the phenomenon comes from.

The Schrödinger operator for this new potential is:

$$\tilde{H}^S(\lambda) = -\Delta + \lambda^2(V(x) + W(x)). \tag{3.63}$$

Similar to the original case, we denote the lowest two eigenvalues of $\tilde{H}^S(\lambda)$ by $\tilde{E}_0^S(\lambda)$ and $\tilde{E}_1^S(\lambda)$. In the same way, $\tilde{\psi}_n$ ($n \in \mathbb{N}$) are the new eigenfunctions and $\tilde{A}(\psi_0)$ is the new vacuum limiting set. The new potential also gives rise to a new Agmon metric ρ_{V+W}. We are interested in

$$a_{ij} = \lim_{\lambda\to\infty} -\lambda^{-1} \ln \left| E_i^S(\lambda) - \tilde{E}_j^S(\lambda) \right|, \tag{3.64}$$

where $i, j \in \{0, 1\}$, and

$$\Delta = \lim_{\lambda\to\infty} -\lambda^{-1} \ln \left| E_1^S(\lambda) - E_0^S(\lambda) \right|, \tag{3.65a}$$

$$\tilde{\Delta} = \lim_{\lambda\to\infty} -\lambda^{-1} \ln \left| \tilde{E}_1^S(\lambda) - \tilde{E}_0^S(\lambda) \right|. \tag{3.65b}$$

We also define some new quantities:

$$d_1 = \min\left[2\rho_V(m_1, \text{supp } W), 2\rho_V(m_2, \text{supp } W)\right]; \tag{3.66a}$$

$$d_2 = \max\left[2\rho_V(m_1, \text{supp } W), 2\rho_V(m_2, \text{supp } W)\right]; \tag{3.66b}$$

$$d = \rho_V(m_1, m_2). \tag{3.66c}$$

The main result of [32] is:

Theorem 3.2.7 (Flea on the Elephant)**.** *Let W be a function satisfying conditions 1-3 above. Also suppose that the conditions in Theorem 3.2.2 hold. In that case:*

1. *if $d < d_1 \le d_2$, then $\Delta = d$, $\tilde{\Delta} = d$, $a_{00} = a_{11} = d_1$, $a_{01} = a_{10} = d$.*
   Furthermore, $\tilde{A}(\psi_0) = \{m_1, m_2\}$.
2. *if $d_1 < d \le d_2$, then $\Delta = d$, $\tilde{\Delta} = d_1$, $a_{00} = a_{10} = d$, $a_{01} = a_{11} = d_1$.*
   Furthermore, $\tilde{A}(\psi_0)$ is one of m_1 and m_2 (the one with $\rho(\cdot, \text{supp } W) = d_2$).
3. *if $d_1 < d_2 < d$, then $\Delta = d$, $\tilde{\Delta} = d_1$, $a_{00} = a_{10} = d_2$, $a_{01} = a_{11} = d_1$.*
   Furthermore, $\tilde{A}(\psi_0)$ is one of m_1 and m_2 (the one with $\rho(\cdot, \text{supp } W) = d_2$).

We can restate part of these conclusions in a more intuitive, but less precise, way:

1. If the perturbation is 'far away from the minima m_1 en m_2', the addition of W does not change anything. The semiclassical ground state continues to be delocalized for all λ.
2. If the perturbation is 'close to one of the minima, but far away from other', the energy splitting changes. The semiclassical ground state localizes to the well that is 'the farthest' from the perturbation as $\lambda \to \infty$.
3. If the perturbation is 'close to both minima', the energy splitting changes. The semiclassical ground state localizes to the well that is 'the farthest' from the perturbation as $\lambda \to \infty$.

Here, the notion of 'distance' is based upon the comparison of d_1 and d_2 with the value $d = \rho_V(m_1, m_2)$.

This can be understood in the following way. The ground state tries to minimize its energy according to the rules:

- The cost of localization is $\mathcal{O}(e^{-\lambda d})$.
- The cost of turning on W is $\mathcal{O}(e^{-\lambda d_1})$ when the wave function is delocalized.
- The cost of turning on W is $\mathcal{O}(e^{-\lambda d_2})$ when the wave function is localized in the well with $\rho(\cdot, \text{supp } W) = d_2$.

Remark 3.2.8. Note that the above conclusions only depend on the points where W is nonzero, but not on the size of $|W(x)|$ at those points. This means that any perturbation can cause localization of the ground state as $\lambda \to \infty$. In the real world, such perturbations will always be present, which implies that localization of the ground state is the natural state of affairs under semiclassical conditions.

3.2.3 One-dimensional double well

The previous result is very general and is applicable in any dimension. We now look at a simple example in one dimension. Consider a symmetric double well potential V in one dimension with an added perturbing potential W that satisfies:

$$\text{supp } W = [a_1, a_2] \subset (0, x_0), \tag{3.67}$$

where x_0 is such that we are dealing with situation 2 or 3 of Theorem 3.2.7. We also assume $a \notin [a_1, a_2]$ and $x_0 > a$. An example of such a situation can be seen in figure 3.4.

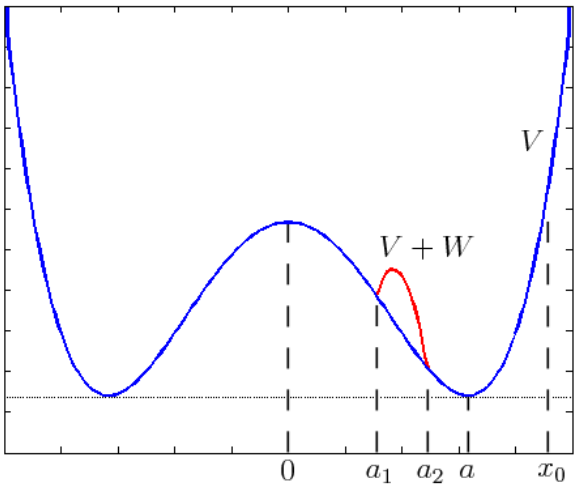

Figure 3.4: An example of a symmetric double well V and perturbed well $V + W$ that satisfy the conditions given above. Note that we are dealing with case 3 of Theorem 3.2.7 here.

Using (3.60), we know that for $\hbar$ sufficiently small:

$$E_1(\hbar) - E_0(\hbar) \approx \hbar \exp\left[-\frac{1}{\hbar}\int_{-a}^{a}(V(s))^{1/2}ds\right]. \tag{3.68}$$

Furthermore, Theorem 3.2.7 tells us that

$$\tilde{E}_1(\hbar) - \tilde{E}_0(\hbar) \approx \hbar \exp\left[-\frac{2}{\hbar}\int_{a_2}^{a}(V(s))^{1/2}ds\right]. \tag{3.69}$$

Realizing that this is valid for mass $m = \frac{1}{2}$, we see that this implies:

$$\frac{(E_1 - E_0)_V}{(E_1 - E_0)_{V+W}} \approx \frac{\exp\left[-\frac{2}{\hbar}\int_0^a (2mV(x))^{1/2}dx\right]}{\exp\left[-\frac{2}{\hbar}\int_{a_2}^a (2mV(x))^{1/2}dx\right]} = \exp\left[-\frac{2}{\hbar}\int_0^{a_2}(2mV(x))^{1/2}dx\right]. \tag{3.70}$$

The mathematical theorems we have discussed do not tell us all there is to know about the wave function. All we have seen is that the ground state localizes to the left and the first excited state localizes to the right in the limit $\hbar \to 0$ (because the perturbation is on the right). Reassuringly, this is in agreement with the conclusions obtained numerically and with the WKB method. It is possible to say more, as is done in [4, 16, 31, 32], but we will not look into it here.

3.3 Comparison

In this section, we compare the results stated in Section 3.1 and Section 3.2, which have been obtained by completely different methods. The physical WKB method provides easy insight in the matter and facilitates calculations. The theorem, however, offers absolute certainty. It would be nice to combine the advantages of these two methods to get a good overview of the problem. Here, we try to do so.

3.3.1 Energy splitting

Our first question is whether the conclusions for the energy splitting of both the perturbed and unperturbed problem agree.

No perturbation

Assume we are dealing with the double well potential in Figure 3.2. Let us summarize our conclusions from the previous sections:

- *Simon* [32] has shown that

$$\lim_{\lambda\to\infty} -\lambda^{-1}\ln\left[E_1(\lambda)-E_0(\lambda)\right] = \int_{-a}^{a}\sqrt{2mV(s)}ds. \tag{3.71}$$

  As in (3.59) and (3.60), we see that this implies for $\hbar$ sufficiently small:

$$\left[E_1(\hbar)-E_0(\hbar)\right]\exp\left[\frac{1}{\hbar}\int_{-a}^{a}\sqrt{2mV(s)}ds\right] = \mathcal{O}(\hbar). \tag{3.72}$$

- *Landau & Lifshitz* [20] approximate the energy splitting by

$$E_1(\hbar)-E_0(\hbar) \approx \frac{\hbar\omega_0}{\pi}\exp\left[-\frac{1}{\hbar}\int_{-x_1}^{x_1}\sqrt{2m\left(V(x)-E_0^{(0)}\right)}dx\right], \tag{3.73}$$

  where $E_0^{(0)}$ is the ground state energy of a single well. The frequency ω_0 is that of a classical particle with energy $E_0^{(0)}$ that oscillates in one of the two wells. It only depends on the shape of the potential, and not on $\hbar$.

- *Garg* [7] corrects this approximation and finds

$$E_1(\hbar)-E_0(\hbar) \approx \frac{\hbar\omega_0}{\sqrt{\pi e}}\exp\left[-\frac{1}{\hbar}\int_{-x_1}^{x_1}\sqrt{2m\left(V(x)-E_0^{(0)}\right)}dx\right]. \tag{3.74}$$

We can now ask whether these results agree. The exponentials seem to be allright. For $\hbar\to 0$, the turning points go down to the minimum of the potential: $x_1 \to a$. The ground state energy of a single well also disappears: $E_0^{(0)} \to 0$. The prefactors of the three results are not the same, but it is still safe to say the results agree. The important thing is that they all have the same $\hbar$-dependence. It is understandable we can not expect a correct physical prefactor from the mathematical result because it ignores dimensions.

Adding a flea

We will now assume the presence of a flea W on the potential, close enough to one of the minima to meet the conditions of either case 2 or case 3 of Theorem 3.2.7. An example of such a situation can be seen in Figure 3.4. If the flea behaves reasonably, the approximations of *Garg* and *Landau & Lifshitz* do not change, since these are valid for a general double well and the perturbation is taken into account by means of the integral.

However, *Simon* finds:

$$\lim_{\lambda\to\infty} -\lambda^{-1}\ln\left[\tilde{E}_1(\lambda)-\tilde{E}_0(\lambda)\right] = d_1 = \min\left[2\rho_V(m_1,\text{supp } W), 2\rho_V(m_2,\text{supp } W)\right];, \tag{3.75}$$

which implies for the actual energies in terms of $\hbar$ (for $\hbar$ sufficiently small):

$$\left[\tilde{E}_1(\hbar)-\tilde{E}_0(\hbar)\right]\exp\left(\frac{d_1}{\hbar}\right) = \mathcal{O}(\hbar). \tag{3.76}$$

There seems to be a problem here: *Simon's* result only depends on the support of the perturbation, but not on its size. However, the WKB result does not really care about the support of the perturbation (as long as it is in $[-x_1, x_1]$), but more about its size. It is uncertain if this actually leads to a discrepancy. It could be that the WKB method is no longer applicable in some cases, which leads to differences in results. Further research is required to confirm this.

3.3.2 Wave function

In the unperturbed case, it is clear that the mathematical and WKB results agree. We should also make a remark about the wave function of a perturbed double well. The most important conclusion is that both approaches show time-independent localization. They also agree as to which side the wave function should collapse in the presence of a perturbation. It is possible, however, to think of situations in which it is not certain whether the two methods agree. An example is given by a perturbation near the top of the barrier, above the energy level at hand. Because the perturbation lies above the energy level, the WKB method (in the way we have used it) does predict localization. Theorem 3.2.7 does, however. Perhaps this can be explained by the limited applicability of our approach in Section 3.1.6 and Section 3.1.7, or the limited applicability of the WKB method in general. Once again, more research is required to find out.

Part II

Time-Dependent Results

Chapter 4

Two-Level System

In Chapter 2, we studied the two-level system with the perturbed Hamiltonian

$$H' = \begin{pmatrix} \Delta V & -\epsilon \\ -\epsilon & 0 \end{pmatrix} \tag{4.1}$$

in a time-independent way. Of course, this is far from the general situation.
Generally, we can look at the time-dependent behaviour of the two-level system in the initial state $\psi(0) = (a, b)$ with the Hamiltonian

$$H(t) = \begin{pmatrix} \Delta V_L(t) & -\epsilon \\ -\epsilon & \Delta V_R(t) \end{pmatrix}, \tag{4.2}$$

where $\Delta V_L(t)$ and $\Delta V_R(t)$ are general perturbations. The behaviour of the system is governed by the Schrödinger equation applied to a general state $\psi(t) = (a(t), b(t))$:

$$i\hbar \ \frac{d}{dt} \begin{pmatrix} a(t) \\ b(t) \end{pmatrix} = H(t) \begin{pmatrix} a(t) \\ b(t) \end{pmatrix}, \qquad \begin{pmatrix} a(0) \\ b(0) \end{pmatrix} = \begin{pmatrix} a \\ b \end{pmatrix}, \qquad |a|^2 + |b|^2 = 1 \ . \tag{4.3}$$

In the coming sections, we will look the behaviour of the two-level system for a number of different choices for these perturbations. For some the calculation can be done analytically, for others we will use numerical methods. Appendix C contains a short outline of the most important numerical method used in this thesis.

In all cases, we are interested in the probability of finding the particle either to the left (P_L) or to the right (P_R), i.e.

$$P_L(t) = |a(t)|^2 \qquad \text{or} \qquad P_R(t) = |b(t)|^2 = 1 - P_L(t) \ . \tag{4.4}$$

Finally, something should be said about the classical limit. In this case, the classical limit $\hbar \to 0$ is often equivalent to very strong noise, i.e. $\Delta V_L(t), \Delta V_R(t) >> \epsilon$. We will use the two limits alternately.

4.1 No perturbation

Let us first look at the time-dependent behaviour of the system when no perturbation is present. In this case, the solution is rather simple:

$$\psi(t) = \frac{1}{\sqrt{2}}(a+b)\psi_0 e^{\frac{i\epsilon t}{\hbar}} + \frac{1}{\sqrt{2}}(a-b)\psi_1 e^{-\frac{i\epsilon t}{\hbar}}, \tag{4.5}$$

where ψ_0 and ψ_1 are defined as in Chapter 2. This means that

$$P_L(t) = |a|^2 + (|b|^2 - |a|^2)\sin^2\left(\frac{\epsilon t}{\hbar}\right), \tag{4.6}$$

so the probability $P_L(t)$ of being 'to the left' oscillates around $P_L = 1/2$ with period $\frac{\pi\hbar}{\epsilon}$. Note that with the expression for the energy splitting (3.36) found in the previous chapter, we see that this period goes to infinity as $\hbar \to 0$. This oscillation has also been observed in a numerical simulation, see Figure 4.1.

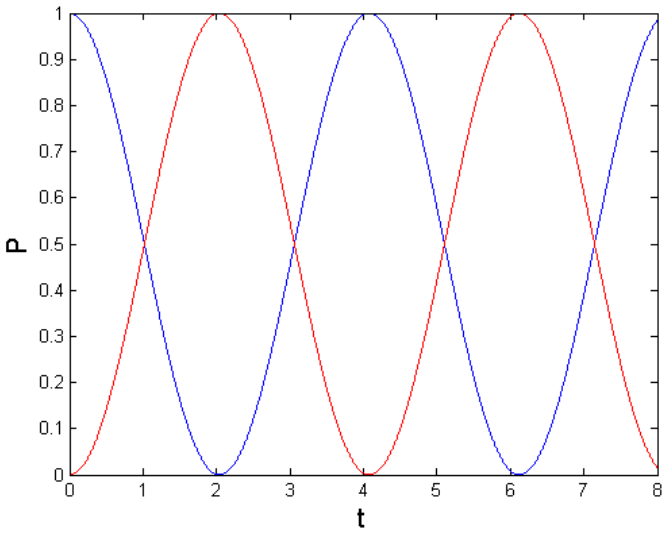

Figure 4.1: Time evolution of the probabilities $P_L(t)$ and $P_R(t)$ for the two-level system without perturbation and initial state ψ_L.

4.2 Constant perturbation

We now consider the time independent Hamiltonian

$$H = \begin{pmatrix} \beta & -\epsilon \\ -\epsilon & -\beta \end{pmatrix}, \tag{4.7}$$

which has eigenvalues

$$\lambda_1 = -\sqrt{\epsilon^2 + \beta^2} \qquad \lambda_2 = \sqrt{\epsilon^2 + \beta^2}, \tag{4.8}$$

and (normalized) eigenvectors

$$v_1 = \left(2\epsilon^2 + 2\beta^2 - 2\beta\sqrt{\epsilon^2+\beta^2}\right)^{-1/2} \begin{pmatrix} -\beta + \sqrt{\epsilon^2+\beta^2} \\ \epsilon \end{pmatrix}, \tag{4.9}$$

$$v_2 = \left(2\epsilon^2 + 2\beta^2 + 2\beta\sqrt{\epsilon^2+\beta^2}\right)^{-1/2} \begin{pmatrix} -\beta - \sqrt{\epsilon^2+\beta^2} \\ \epsilon \end{pmatrix}. \tag{4.10}$$

With a Taylor expansion, one sees that in the limit of very strong noise ($\beta >> \epsilon$):

$$v_1 \to \begin{pmatrix} 0 \\ 1 \end{pmatrix}, \tag{4.11}$$

$$v_2 \to \begin{pmatrix} -1 \\ 0 \end{pmatrix}. \tag{4.12}$$

Therefore, the limit of very strong noise (which is the classical limit) leads to localization of the eigenvectors (i.e. time-independent localization) as for the comparable Hamiltonian discussed in Chapter 2. We now investigate the behaviour of the system for a given initial state

$$\psi(0) = \begin{pmatrix} a \\ b \end{pmatrix}, \tag{4.13}$$

where $a, b \in \mathbb{C}$. Since the Hamiltonian is time-independent, the solution is simply

$$\psi(t) = c_1 e^{\frac{-i\lambda_1}{\hbar}t} v_1 + c_2 e^{\frac{-i\lambda_2}{\hbar}t} v_2 \ , \tag{4.14}$$

where the coefficients c_1 and c_2 are determined by the initial state $\psi(0)$:

$$c_1 = \langle \psi(0), v_1 \rangle \, , \qquad\qquad c_2 = \langle \psi(0), v_2 \rangle \, . \tag{4.15}$$

This means that for given ϵ, β the solution oscillates with frequency $\sqrt{\epsilon^2 + \beta^2}/(\pi\hbar)$.
It is possible to calculate what this means for the probability for being left or right. For example, the probability for the state being on the left for $a, b \in \mathbb{R}$ is

$$P_L(t) = c_1^2 d_1^2 + c_2^2 d_2^2 + \frac{(b^2 - a^2)\epsilon^2 - 2ab\epsilon\beta}{2(\epsilon^2 + \beta^2)} \cos\left(\frac{\sqrt{\epsilon^2 + \beta^2}}{\hbar} t \right), \tag{4.16}$$

where d_1 and d_2 are constants depending on ϵ and β such that $P_L(0) = |a|^2$. The important thing to notice here is the fact that the amplitude goes to zero in the limit of very strong noise ($\beta >> \epsilon$). Furthermore, the equillibrium position goes to $|a|^2$. This means that the oscillation disappears for very strong noise (i.e. the classical limit), and the system freezes in its initial position. In fact, any initial state $\psi(0)$ leads to an oscillation with diminishing amplitude for very strong noise. This means that in the limit of very strong noise, there is no localization: the system simply remains in its original position. This is also supported by numerical results.

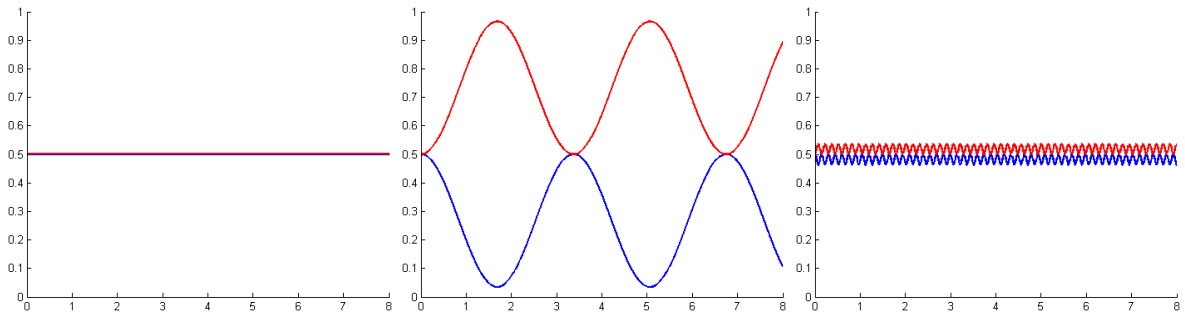

(a) $\beta = 0$ (b) $\beta = \beta_b < \beta_c$ (c) $\beta = \beta_c > \beta_b$

Figure 4.2: Time evolution of the probabilities $P_L(t)$ and $P_R(t)$ for the two-level system with Hamiltonian (4.7) and the initial delocalized state ψ_0 (defined in Chapter 2) for different β. The first image has no noise, the second has moderate noise and the third has strong noise. For strong noise, the system remains frozen in its initial state. The numerical simulations show this 'freezing effect' for every initial state.

4.3 Slowly rising perturbation

We have also looked at the following perturbation for $t \in [0, T],\ T > 0$:

$$\Delta V_L(t) = \beta \sin\left(\frac{\pi t}{2T}\right), \qquad \Delta V_R(t) = -\beta \sin\left(\frac{\pi t}{2T}\right). \tag{4.17}$$

This is a slowly rising perturbation in the left well and a slowly lowering one in the right well. A sample time evolution for such an Hamiltonian can be seen in Figure 4.3. For moderate β, we indeed see localization, but for $\beta \to \infty$ and T fixed, this effect disappears and the system freezes in its original position once again. However, if things are the other way around, i.e. β is fixed and T becomes large, we do see time-dependent localization. This is also predicted by the adiabatic approximation, which we will discuss in Section 5.3.

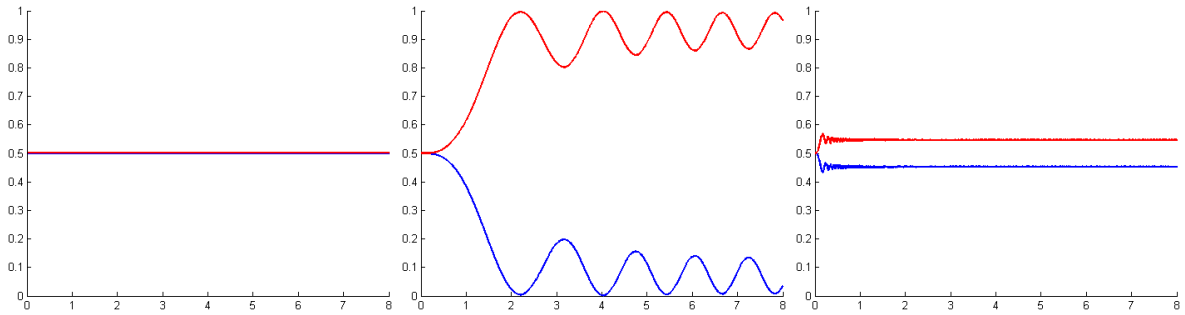

(a) $\beta = 0$ (b) $\beta = \beta_b < \beta_c$ (c) $\beta = \beta_c > \beta_b$

Figure 4.3: Time evolution of the probabilities $P_L(t)$ and $P_R(t)$ for the two-level system with Hamiltonian (4.2) with (4.17) and the initial delocalized state ψ_0 (defined in Chapter 2) for different β and fixed T. The first image has no noise, the second has moderate noise and the third has strong noise. For $\beta = \beta_c$, the system freezes to a state different from the initial state, but this becomes the initial state in the limit $\beta \to \infty$. As in Section 4.2, the numerical simulations show this 'freezing effect' for every initial state.

4.4 Classical Noise

The previous two choices for the perturbation in (4.2) did not involve any random effects. This made both calculations and simulations easy, but it is not very realistic. In a realistic situation, we expect perturbations to be of random nature. We will now consider two such perturbations: *Poisson noise* and *white noise*. Both of these are *classical noises*: they are typically caused by a classical environment (e.g. a heat bath), and they do not involve any quantum uncertainties. This section aims to introduce these two kinds of classical noise, based on [18]. In that reference, it is also shown that white noise and Poisson noise are sufficient to produce all classical noises. That means if suffices to study these two kinds of noise to say something about the effect of classical noise in general. In later sections, we will do this both analytically and numerically.

First, we need a basic definition to make clear how we can make a stochastic object like noise depend on time.

Definition 4.4.1. Suppose we have a probability space (Ω, F, P), where Ω is a sample space containing all possible outcomes, X is a σ-algebra containing events and P is a probability measure on X. A *stochastic process* with state space X is a collection of X-valued random variables on Ω indexed by a set T ('time'). That is, a stochastic process is a collection $\{A_t \mid t \in T\}$, where A_t is an X-valued random variable on Ω for each $t \in T$.

Noise is a stochastic process. If we would perform a single measurement on the system, we would see one particular manifestation of this noise (i.e. a draw from the stochastic process). That means the outcome of a measurement is different each time, which makes it difficult to predict the outcome of an

individual case. However, it is possible to say something about the expectation value of the outcome. This expectation value depends on the properties of both the system and the noise added to it. Now that we have made clear how noise depends on time, let us look at the properties of the two kinds of classical noise.

4.4.1 Poisson Noise

We would like to model a noise process that generates random point-like events (*clicks*) in a certain time interval $[0, T]$. A physical interpretation of such a click would be some particle that comes by, interacts with our system and disturbs it very briefly. The outcome of the process is a finite set

$$\omega = \{t_1, t_2, \ldots, t_n\},$$

for which we will assume

$$0 \leq t_1 < t_2 < \ldots < t_n \leq T \ . \tag{4.18}$$

To characterize this process, we will look for a probability measure μ on the set of all possible outcomes, i.e. on

$$\Delta[0, T] = \bigcup_{n=0}^{\infty} \Delta_n[0, T], \tag{4.19}$$

where $\Delta_0[0, T] = \{\emptyset\}$ (no clicks) and $\Delta_n[0, T]$ is isomorphic to that part of $[0, T]^n$ where (4.18) holds (n clicks). A natural measure on $\Delta[0, T]$, which we denote by $d\omega$, is defined by

$$\int_{\Delta_0[0,T]} d\omega = 1 \qquad \text{and} \qquad \int_A d\omega = \int_A dt_1 \ldots dt_n, \tag{4.20}$$

where $dt_1 \ldots dt_n$ is the Lebesgue measure carried over from $[0, T]^n$ to $\Delta_n[0, T]$, and $A \subset \Delta_n[0, T]$ is assumed Lebesgue measurable.

The random variable N_t counts the amount of clicks that occured before or at time $t \in [0, T]$:

$$N_t : \quad \omega \longmapsto |\omega \cap [0, t]| \ .$$

When we combine these random variables we get a stochastic process $(N_t)_{0 \leq t \leq T}$. The number of clicks that occur in the interval $(s, t]$, for $t > s$, is equal to the *increment* $N_t - N_s$ of the stochastic process.

To model noise correctly, we would like the process to have the properties:

1. The number of clicks during a certain time interval depends only on the length of the interval. That is: for $0 \leq s < t \leq T$ the probability distribution of $N_t - N_s$ depends only on $t - s$.
   In this case, we say that the process $(N_t)_{0 \leq t \leq T}$ has *stationary increments*.

2. The increments over any finite collection of disjoint time intervals are independent.
   In this case, we say that the process $(N_t)_{0 \leq t \leq T}$ has *independent increments*.

3. The expectation number of the total number of clicks is λT, for some $\lambda > 0$.

It turns out such a process exists and is fully characterized by these properties. The following theorem proved in [18] gives three equivalent characterizations.

Theorem 4.4.2 (Characterizations of the Poisson measure)**.** *Let $\lambda, T > 0$. For a probability measure μ on $\Delta[0, t]$ the following conditions are equivalent:*

- *The process $(N_t)_{0 \leq t \leq T}$ has stationary independent increments and $\mathbb{E}_\mu(N_T) = \lambda T$.*
- *The process $(N_t)_{0 \leq t \leq T}$ has stationary independent increments and for each $t \in [0, T]$, N_t has a Poisson distribution with parameter λt.*
- *For any measurable subset A of $\Delta_n[0, T]$, we have $\mu(A) = \lambda^n e^{-\lambda T} \int_A d\omega$.*

This is known as a *Poisson process* with parameter λ. To generate such a Poisson process numerically, we have used the following corollary of this theorem.

Corollary 4.4.3. *Let $(N_t)_{0\leq t\leq T}$ be a Poisson process with parameter λ.*
Denote by S the random variable given by

$$S: \quad \omega \longmapsto t_1.$$

Then S has an exponential distribution with parameter $\frac{1}{\lambda}$.

Proof. Let $T > t_1 > 0$. We want to know the probabilty that at least one click has arrived at t_1. Since N_{t_1} is Poisson distributed with parameter λt_1, this probability is

$$\mathbb{P}[N_{t_1} \geq 1] = 1 - e^{-\lambda t_1}.$$

This is exactly the Cumulative Distribution Function (CDF) $F_S(t_1)$ of T, since it gives the probability that S has a value below t_1. So the probability density function (pdf) of S is

$$f_S(t_1) = \lambda e^{-\lambda t_1},$$

and therefore, S has an exponential distribution with parameter $\frac{1}{\lambda}$. □

Remark 4.4.4. To generate a set of clicks, we can make a draw out of an exponential distribution with parameter $\frac{1}{\lambda}$ to get the time t_1 of the first click. Because the increments are independent, we can make another draw and add the result to t_1 to get the time of the second click t_2. We have used this to model Poisson process numerically.

4.4.2 White Noise and Brownian Motion

The second kind of classical noise we study is *white noise*. We would like it to be some stochastic process (A_t) that models 'truly random' noise. For this purpose, the following properties seem reasonable:

1. A_t is independent of A_s for $t \neq s$.
2. All random variables A_t $(t \geq 0)$ have the same probability distribution.
3. $\mathbb{E}(A_t) = 0$.

Unfortunately, it turns out that no such process can be constructed in a satisfying way. A process that meets these conditions is not measurable in t, unless it is identically zero. To be able to characterize white noise, we first have to introduce a stochastic process known as *Brownian motion* or *Wiener process* in $\mathbb{R}$. Unlike white noise, this process can be defined in a satisfying way.

Let $C_0[0,T]$ denote the set of all continuous functions $\omega: [0,T] \longrightarrow \mathbb{R}$ so that $\omega(0) = 0$. The random variable B_t evaluates the function ω at $t \in [0,T]$:

$$B_t: \quad \omega \longmapsto \omega(t).$$

Therefore, $C_0[0,T]$ is the space of all possible outcomes of the process $(B_t)_{0\leq t\leq T}$. Once again, we have some properties we would like $(B_t)_{0\leq t\leq T}$ to have:

1. The process $(B_t)_{0\leq t\leq T}$ has stationary increments.
2. The process $(B_t)_{0\leq t\leq T}$ has independent increments.
3. For any $t \in [0,T]$, B_t has mean 0 and variance $\sigma^2 t$.

In this case, it turns out such a process does exists and is fully characterized by these properties. The following theorem gives an equivalent formulation, and is partially proven in [18].

Theorem 4.4.5 (Characterizations of Brownian motion)**.** *Let $\sigma, T > 0$. For a probability measure μ_0 on $C_0[0,T]$ the following conditions are equivalent:*

- *The process $(B_t)_{0\leq t\leq T}$ has stationary independent increments and for each $t \in [0,T]$, the random variable B_t has mean 0 and variance $\sigma^2 t$.*
- *The process $(B_t)_{0\leq t\leq T}$ has stationary independent increments and for each $t \in [0,T]$, the random variable B_t has Gaussian distribution with mean 0 and variance $\sigma^2 t$.*

This is known as *Brownian motion* with variance σ^2. Physically, this process has been used to describe the motion of a particle suspended in a fluid [5]. Because of the atoms that collide with the particle, it appears to move in a random way along a continuous path. Figure 4.4 shows such a random walk. The random variable B_t represents the location of the particle at time t.

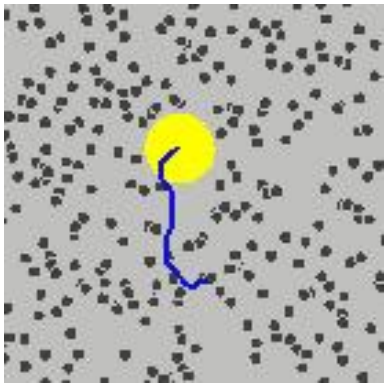

Figure 4.4: The motion of a large particle (yellow) which is subject to white noise caused by the motion of atoms in a fluid (gray). The resulting path (blue) is a draw from the Brownian motion $(B_t)_{0\leq t\leq T}$. This image has been taken from the Wikipedia page on Brownian motion.

Now consider the ideal properties of white noise formulated at the beginning of this subsection. Brownian motion does not have the first property: a particle's location at a certain time is not independent of its location at some earlier time. However, when one thinks about it in an intuitive way, the 'steps' of a particle in Brownian motion do seem to have this property. In an infinitisimal sense, these 'steps' are linked to the 'derivative' of Brownian motion. Therefore, *white noise* A_s is formally defined as the derivative of Brownian motion, i.e. '$A_t = \frac{dB_t}{dt}$', or more correct,

$$B_t = \int_0^t A_s ds. \tag{4.21}$$

A precise definition of white noise can be found in [25].

Remark 4.4.6. For the numerical simulation of white noise, it is important to realize that the Schrödinger equation is solved by calculating the state of a system at a finite number of times (which is explained in Appendix C). That means we do not need to consider a precise definition of white noise, since it is not possible to implement it anyway. Instead, it is better to consider the preferred properties of white noise stated at the beginning of this subsection. These can be achieved in the following way: at any of the considered points in time, a draw is made from a fixed normal distribution with mean 0. The variance of this normal distribution is a measure of the strength of the noise. That way, white noise can easily be modelled numerically.

4.5 Stochastic Calculus

The aim of this chapter is to add a perturbation to the two-level system and see what the time-evolution as dictated by the Schrödinger equation looks like. For stochastic perturbations such as white noise and Poisson noise, we can no longer use ordinary calculus to solve the Schrödinger equation. A tool that is fit for the job is *stochastic calculus*, which considerably differs from the usual calculus. Much like a first lecture in ordinary calculus, we will give a short overview of the rules of calculation that stochastic calculus allows. A rigorous treatment requires stochastic analysis and can be found in [25].

To deal with white noise, we use a result known as *Itô's Lemma*. It allows us to calculate time derivatives of stochastic processes that involve Brownian motion, and may be seen as the equivalent of the chain rule in normal calculus. Itô's Lemma forms the basis of the theory of *stochastic differential equations*, which is widely used in physics and finance. A proof and statement of the general theorem can be found in [25]. Here, we state a simplified version in one dimension.

Theorem 4.5.1 (Itô's Lemma)**.** *Let $(B_t)_{0\leq t\leq T}$ be Brownian motion. Let $g : [0,\infty) \times \mathbb{R} \to \mathbb{R}$ be twice continuously differentiable. Then the process $X_t \equiv g(t, B_t)$ statifies*

$$dX_t = \frac{\partial g}{\partial t}(t, B_t)\ dt + \frac{\partial g}{\partial B_t}(t, B_t)\ dB_t + \frac{1}{2}\frac{\partial^2 g}{\partial B_t^2}(t, B_t)\ dt\ . \tag{4.22}$$

Here, the derivatives with respect to B_t should be treated as if B_t were just some variable.

It is the last term in dX_t that is surprising and is different from normal calculus.
We require some more results from stochastic calculus presented in [25]:

- $dt^2 = dtdB_t = dB_t dt = 0$,
- $dB_t^2 = dt$,
- $\overline{dB_t} = 0$, which is the expectation value of dB_t. Intuitively, this make sense because of (4.21) and the properties of white noise.
- $\overline{dt} = dt$, since there is nothing stochastic about dt.

We now apply these facts to the Schrödinger equation for some stochastic Hamiltonian of a two-level system.

Example 4.5.2. Consider the following Hamiltonian, which contains Pauli spin matrices:

$$H(t) = \begin{pmatrix} \beta A_t & -\epsilon \\ -\epsilon & -\beta A_t \end{pmatrix} = -\epsilon\sigma_x + \beta A_t \sigma_z, \tag{4.23}$$

where A_t is white noise. By the Schrödinger equation, we know that the time evolution of the wave function $\psi(t)$ is given by

$$\psi(t) = \exp\left[-i\int_0^t H(s)ds\right]\psi(0), \tag{4.24}$$

where we have ignored a factor $\hbar$ to bring our results into agreement with [2]. To obtain a physically correct result, one should make the substitutions $\epsilon \to \frac{\epsilon}{\hbar}$ and $\beta \to \frac{\beta}{\hbar}$. Note that this does not change the nature of the classical limit in the formulas used, since that limit corresponds to $\beta/\epsilon \to \infty$. By calculating the integral using (4.21), we see that

$$\psi(t) = \exp\left[i\epsilon\sigma_x t - i\beta\sigma_z B_t\right]\psi(0)\ . \tag{4.25}$$

By Theorem 4.5.1, this leads to the stochastic Schrödinger equation

$$d\psi = i\epsilon\sigma_x\psi\ dt - i\beta\sigma_z\psi\ dB_t - \frac{1}{2}\beta^2\psi\ dt, \tag{4.26}$$

The result of this example will be used in Section 4.6. It fits in the broader framework of *essentially commutative dilations on M_n*, as described in [19]. These dilations are mixtures of Brownian motion and Poisson processes on the automorphism group $\mathrm{Aut}(M_n)$ of the $n \times n$-matrices. Physically speaking, they describe quantum mechanical evolution caused by a classical environment. In this example, such a classical environment is the cause of the white noise present in the Hamiltonian.

For Poisson noise, we will not use Theorem 4.5.1 to derive $d\psi$ from the Hamiltonian. Instead, we immediately state the stochastic Schrödinger equation for a Poisson perturbed system in Section 4.8. Moreover, it is important to know that for a Poisson process N_t with parameter λ, we have

$$\overline{dN_t} = \lambda \, dt, \tag{4.27}$$

which follows from the first characterization of the Poisson process in Theorem 4.4.2. But what does Poisson noise look like? It can be seen as the influence of atoms that interact with the system [26]. Once in a while, such an atom comes by and disturbes the system, which causes the state to make a jump. Such a stochastic process is known as a *Poisson jump process*.

4.6 White Noise

Now that we have looked at some theory, it is time to turn to actual results. In this section, we consider the Hamiltonian (4.23). We analyze this Hamiltonian both stochastically and numerically to see what happens in the classical limit $\beta/\epsilon \to \infty$. These two methods complement each other nicely. The former is precise, but it can only say something about ensemble averages. In terms of Schrödinger's Cat, that means: multiple boxes each with a cat (and fleas). This will make it difficult to say something about a particular case, as we will see later. The latter is less precise, because it is of a numerical nature and hence approximative. However, it is capable of showing us a single realization of the experiment, i.e. one cat in one box.

4.6.1 Calculation

This calculation is based on [2, 22], where this system has been studied as well. As we have seen in Example 4.5.2, the Hamiltonian (4.23) corresponds to the following Schrödinger equation:

$$d\psi = i\epsilon\sigma_x\psi \, dt - i\beta\sigma_z\psi \, dB_t - \frac{1}{2}\beta^2\psi \, dt, \tag{4.28}$$

where we use $\psi = (\psi_+, \psi_-)^t$ in the usual way, and B_t is the Brownian motion associated with A_t.
To solve this equation, we introduce the vector

$$L = (\psi^*)^t\sigma\psi = (\psi^*)^t(\sigma_x, \sigma_y, \sigma_z)\psi = (x, y, z). \tag{4.29}$$

The terms of L are:

$$x = 2\mathrm{Re}\left[\psi_+^*\psi_-\right], \tag{4.30}$$
$$y = -2\mathrm{Im}\left[\psi_+^*\psi_-\right], \tag{4.31}$$
$$z = |\psi_+|^2 - |\psi_-|^2, \tag{4.32}$$

supplemented by the normalization condition $|\psi_+|^2+|\psi_-|^2 = 1$. Note that the crucial entry of L is z, since that one indicates localization. To calculate the differential of L, we apply the general (multidimensional) version of Itô's Lemma as formulated in [25]. This leads us to:

$$dL = (d\psi^*)^t\sigma\psi + (\psi^*)^t\sigma d\psi + (d\psi^*)^t\sigma d\psi = 2\mathrm{Re}\left[(\psi^*)^t\sigma d\psi\right] + (d\psi^*)^t\sigma d\psi. \tag{4.33}$$

Note that once again an unexpected final term appears. The above equation together with the rules for multiplications of differentials stated earlier imply that the Schrödinger equation (4.28) leads to the following equation for dL:

$$dL = DL \, dt + EL \, dB_t, \tag{4.34}$$

where

$$D = \begin{pmatrix} -2\beta^2 & 0 & 0 \\ 0 & -2\beta^2 & 2\epsilon \\ 0 & -2\epsilon & 0 \end{pmatrix} \qquad \text{and} \qquad E = \begin{pmatrix} 0 & -2\beta & 0 \\ 2\beta & 0 & 0 \\ 0 & 0 & 0 \end{pmatrix}. \tag{4.35}$$

Taking expectation values on both sides, we see that

$$d\overline{L} = D\overline{L}\ dt \qquad \text{so} \qquad \frac{d}{dt}\overline{L} = D\overline{L}, \tag{4.36}$$

since $\overline{dB_t} = 0$, as mentioned before.
To solve this equation, we must distinguish two cases: $\beta^2 < 2|\epsilon|$ and $\beta^2 > 2|\epsilon|$. We are interested in the classical limit, which is equivalent to the limit $\beta/\epsilon \to \infty$. That is why we only consider the second case, whereas [2] focuses on the first. After some calculation, the following solution for the expectation value of L in the regime $\beta^2 > 2|\epsilon|$ is found:

$$\overline{x(t)} = e^{-2t\beta^2}\overline{x(0)}\ ; \tag{4.37}$$

$$\overline{y(t)} = e^{-t\beta^2}\left[\overline{y(0)}\cosh(\omega t) + c_1 \sinh(\omega t)\right]; \tag{4.38}$$

$$\overline{z(t)} = e^{-t\beta^2}\left[\overline{z(0)}\cosh(\omega t) + c_2 \sinh(\omega t)\right], \tag{4.39}$$

with

$$\begin{aligned}
\omega &= |\beta^4 - 4\epsilon^2|^{1/2}\ ; \\
c_1 &= \frac{1}{\omega}\left[-\beta^2\overline{y(0)} + 2\epsilon\overline{z(0)}\right]; \\
c_2 &= \frac{1}{\omega}\left[\beta^2\overline{z(0)} - 2\epsilon\overline{y(0)}\right].
\end{aligned}$$

Note that the average is taken over the stochastic process; it is not a time average. We are interested in the regime of very strong noise, which is $\beta/\epsilon \to \infty$. The classical limit implies $\beta^2 >> 2|\epsilon|$, which we can easily apply to the previous result.[1] In this case $\omega \to \beta^2$, $c_1 \to -\overline{y(0)}$ and $c_2 \to \overline{z(0)}$, which means

$$\overline{x(t)} = e^{-2t\beta^2}\overline{x(0)}; \tag{4.40}$$

$$\overline{y(t)} = e^{-2t\beta^2}\overline{y(0)}; \tag{4.41}$$

$$\overline{z(t)} = \overline{z(0)}. \tag{4.42}$$

Since z denoted the localization, we conclude that the ensemble average of the localization is exactly the initial localization. What does this say about actual localization? Unfortunately, not as much as we would want, as can be demonstrated by an example. Suppose $z(0) = 0$, which is the case when the initial state is the (delocalized) ground state. In that case, we know that $\overline{z(t_1)} = 0$ for any time t_1. It could be that $z(t_1) = \pm 1$ with equal probability, since that would imply $\overline{z(t_1)} = 0$. It could also be that it is still in the ground state in every realization at time t_1, since that would also imply $\overline{z(t_1)} = 0$. Of course, any combination of these two cases is also possible.

There is one case in which we can actually say something, namely $z(0) = \pm 1$. Since $z(t) \in [-1, 1]$, the fact that $\overline{z(t)} = \pm 1$ implies that $z(t) = \pm 1$ for all t. We therefore see that an initially localized state remains localized in this limit, i.e. strong noise 'freezes' the initial state. But why would the initial states with $z(0) = \pm 1$ be special? Perhaps any state freezes in this way. There is a way to check this: we can use numerical techniques to look at single realizations of the process. The results are discussed in the next subsection.

[1] To see that the classical limit implies $\beta^2 >> 2|\epsilon|$, one should consider the correct $\hbar$-dependence of ϵ and β discussed in Example 4.5.2.

4.6.2 Numerical results

In order to obtain numerical results, we have generated white noise as discussed in Remark 4.4.6. We then added it to the Hamiltonian and solved the Schrödinger equation as described in Appendix C. This yields pictures like in Figure 4.5.

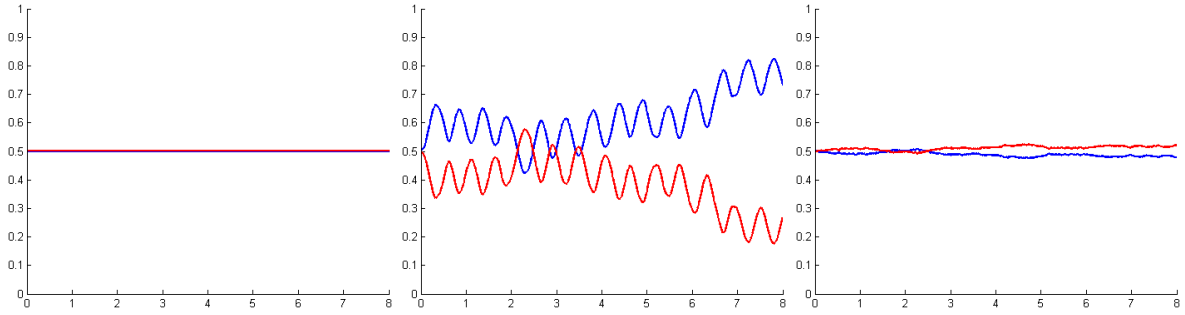

(a) $\beta = 0$ (b) $\beta = \beta_b < \beta_c$ (c) $\beta = \beta_c > \beta_b$

Figure 4.5: Time evolution of the probabilities $P_L(t)$ and $P_R(t)$ for the two-level system with Hamiltonian (4.23) and the initial delocalized state ψ_0 for different β. The first image has no noise, the second has moderate noise and the third has strong noise. For strong noise, the system remains frozen in its initial state as before. The simulations show this 'freezing effect' for every inital state.

So our presumption about the system to freeze in its initial state is supported by numerical evidence. Also note that the results of analytic calculation and simulation are in agreement. It is not the result, however, we expect from an accurate model for Schrödinger's Cat, since a delocalized state remains delocalized. Later, we will discuss this discrepancy in more depth.

4.7 Different white noise in the two wells

We now replace the Hamiltonian (4.23) with

$$H(t) = \begin{pmatrix} 2\beta_1 A_t^{(1)} & -\epsilon \\ -\epsilon & 2\beta_2 A_t^{(2)} \end{pmatrix} = -\epsilon\sigma_x + \beta_1 A_t^{(1)}(1+\sigma_z) + \beta_2 A_t^{(2)}(1-\sigma_z), \tag{4.43}$$

that is, we decouple the noise in both of the wells. The motivation for this is the following: the 'flea on the elephant'-result (Theorem 3.2) tells us to which side the ground state will collapse (time-independently), given a single perturbation. To which side this is, depends on the location of the perturbation. We therefore want to separate the perturbations on the 'left' and on the 'right'.

4.7.1 Calculation

The new Hamiltonian leads to a new Schrödinger equation in the same way as before:

$$d\psi = i\epsilon\sigma_x\psi\, dt - i\beta_1(1+\sigma_z)\psi\, dB_t^{(1)} - \frac{1}{2}\beta_1^2(1+\sigma_z)^2\psi\, dt - i\beta_2(1-\sigma_z)\psi\, dB_t^{(2)} - \frac{1}{2}\beta_2^2(1-\sigma_z)^2\psi\, dt\,. \tag{4.44}$$

That, in turn, leads to a new equation for dL:

$$dL = D'L\, dt + E'L\, dB_t^{(1)} dB_t^{(2)} + F_1 L\, dB_t^{(1)} + F_2 L\, dB_t^{(2)}, \tag{4.45}$$

where

$$D' = \begin{pmatrix} -2(\beta_1^2+\beta_2^2) & 0 & 0 \\ 0 & -2(\beta_1^2+\beta_2^2) & 2\epsilon \\ 0 & -2\epsilon & 0 \end{pmatrix}, \qquad E' = \begin{pmatrix} 4\beta_1\beta_2 & 0 & 0 \\ 0 & 4\beta_1\beta_2 & 0 \\ 0 & 0 & 0 \end{pmatrix},$$

$$F_1 = \begin{pmatrix} 0 & -2\beta_1 & 0 \\ 2\beta_1 & 0 & 0 \\ 0 & 0 & 0 \end{pmatrix}, \qquad F_2 = \begin{pmatrix} 0 & 2\beta_2 & 0 \\ -2\beta_2 & 0 & 0 \\ 0 & 0 & 0 \end{pmatrix}.$$

Note that this equation gives (4.34) when $B_t^{(1)} = B_t^{(2)} = B_t$, $\beta_1 = \frac{1}{2}\beta$ and $\beta_2 = -\frac{1}{2}\beta$, which is of course as desired. Using the fact that $\overline{dB_t^{(1)}} = \overline{dB_t^{(2)}} = \overline{dB_t^{(1)} dB_t^{(2)}} = 0$, we see that

$$d\overline{L} = D'\overline{L}\, dt \qquad \text{so} \qquad \frac{d}{dt}\overline{L} = D'\overline{L}. \tag{4.46}$$

Therefore, we obtain exactly the same result as earlier, with $\beta = \sqrt{\beta_1^2 + \beta_2^2}$. Of course, our conclusion also remains the same.

4.7.2 Numerical results

The conclusion that the Hamiltonian (4.43) leads to the same behaviour as the system discussed in Section 4.6 is supported by numerical evidence. An example can be seen in Figure 4.6.

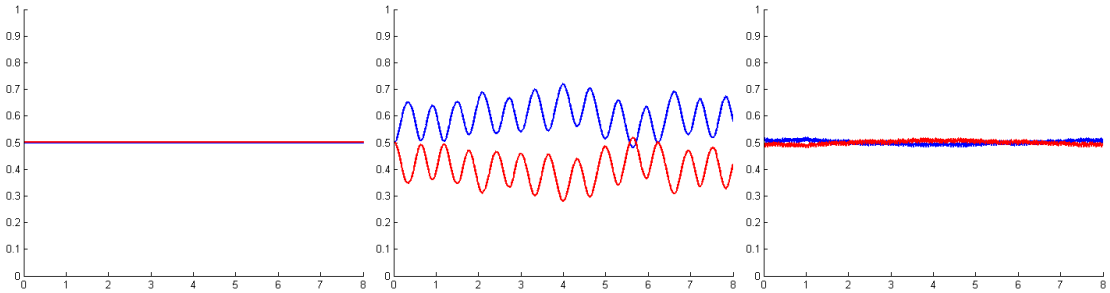

(a) $\beta = 0$ (b) $\beta = \beta_b < \beta_c$ (c) $\beta = \beta_c < \beta_b$

Figure 4.6: Time evolution of the probabilities $P_L(t)$ and $P_R(t)$ for the two-level system with Hamiltonian (4.43) and the initial delocalized state ψ_0 for different $\beta_1 = \beta_2 = \beta$. The first image has no noise, the second has moderate noise and the third has strong noise. For strong noise, the system remains frozen in its initial state. The simulations show this 'freezing effect' for every inital state.

4.8 Poisson noise

We now study a two-level system that is disturbed by Poisson noise. The Schrödinger equation describing such a system is

$$d\psi = i\epsilon\sigma_x\psi dt - (U - I)\psi dN_t, \tag{4.47}$$

where N_t is a Poisson process with parameter λ, and U is some unitary tranformation [26]. As remarked earlier, Poisson noise can be seen as the disturbance caused by a passing particle that interacts with our system for a brief moment. This interaction causes the state of our system to make a jump. How often this happens is dictated by the parameter λ, and the unitary transformation U describes the nature of the jump. In reality, U is different for each particle that comes by. However, we will only consider fixed U here.

4.8.1 Calculation

We will solve this equation for $U \in \{I, \sigma_x, \sigma_y, \sigma_z\}$ to get an idea of what can happen. During the calculation, we will use the fact that that

$$\overline{dN_t} = \lambda\, dt, \tag{4.48}$$

by the properties of a Poisson process.

- $U = I$
  In this case the Poisson proces does not play any role since it disappears from the Schrödinger equation (4.47). After some calculation we see that:

$$dL = DL\ dt, \tag{4.49}$$

  where

$$D = \begin{pmatrix} 0 & 0 & 0 \\ 0 & 0 & 2\epsilon \\ 0 & -2\epsilon & 0 \end{pmatrix}, \tag{4.50}$$

  which is also true for the expectation value $\overline{L(t)}$.
  As expected, this leads to the usual oscillating behaviour for z:

$$z(t) = c\sin(2\epsilon t) + \overline{z(0)}\cos(2\epsilon t), \tag{4.51}$$

  where c is a constant. Although no localization takes place, one should note that ϵ is connected to energy splitting of the double well potential found in chapter 3, which implies that the oscillating frequency goes to zero as $\hbar$ does.

- $U = \sigma_x$
  This time we keep the Poisson term in (4.47).
  A calculation yields:

$$dL = DL\ dt + EL\ dN_t, \tag{4.52}$$

  where

$$D = \begin{pmatrix} 0 & 0 & 0 \\ 0 & 0 & 2\epsilon \\ 0 & -2\epsilon & 0 \end{pmatrix} \qquad \text{and} \qquad E = \begin{pmatrix} 0 & 0 & 0 \\ 0 & -2 & 0 \\ 0 & 0 & -2 \end{pmatrix}.$$

  In terms of expectation values, this means

$$d\overline{L} = F\overline{L}\ dt, \tag{4.53}$$

  where

$$F = \begin{pmatrix} 0 & 0 & 0 \\ 0 & -2\lambda & 2\epsilon \\ 0 & -2\epsilon & -2\lambda \end{pmatrix}.$$

  This can easily be solved:

$$\overline{x(t)} = \overline{x(0)}; \tag{4.54}$$

$$\overline{y(t)} = e^{-2\lambda t}\left[\cos(2\epsilon t)\overline{y(0)} + \sin(2\epsilon t)\overline{z(0)}\right] \tag{4.55}$$

$$\overline{z(t)} = e^{-2\lambda t}\left[\cos(2\epsilon t)\overline{z(0)} - \sin(2\epsilon t)\overline{y(0)}\right]. \tag{4.56}$$

  In the limit of very strong noise ($|\lambda| >> |\epsilon|$), this means that $\overline{z(t)} \to 0$. As before, we cannot conclude anything about the localization: if the system is delocalized every time (i.e. for every sample $z(t) = 0$), we find $\overline{z(t)} = 0$, but if it is localized with probability 1/2 on either side (i.e. for every sample $z(t) = \pm 1$ with equal probability) we also find $z(t) = 0$. Of course, any combination of these two options is also possible.

- $U = \sigma_y$
  Here, we immediately state the conclusion for the expection value:

$$d\overline{L} = F\overline{L}\ dt, \tag{4.57}$$

with

$$F = \begin{pmatrix} -2\lambda & 0 & 0 \\ 0 & 0 & 2\epsilon \\ 0 & -2\epsilon & -2\lambda \end{pmatrix}.$$

Note that this resembles the problem and solution in (4.35)-(4.39) with the following adaptations

$$\begin{aligned} \beta^2 &\to \lambda; \\ \epsilon &\to -\epsilon; \\ (\overline{x}, \overline{y}, \overline{z}) &\to (\overline{x}, \overline{z}, \overline{y}). \end{aligned}$$

This leads to the following result for $\lambda >> 2|\epsilon|$:

$$\overline{x(t)} = e^{-2t\lambda}\overline{x(0)}; \tag{4.58}$$

$$\overline{y(t)} = \overline{y(0)}; \tag{4.59}$$

$$\overline{z(t)} = e^{-2t\lambda}\overline{z(0)}. \tag{4.60}$$

Once again, there is no localization.

- $U = \sigma_z$

Again, we state the conclusion for the expectation value right away:

$$d\overline{L} = F\overline{L}\ dt, \tag{4.61}$$

with

$$F = \begin{pmatrix} -2\lambda & 0 & 0 \\ 0 & -2\lambda & 2\epsilon \\ 0 & -2\epsilon & 0 \end{pmatrix}.$$

Once more, this resembles the problem and solution in (4.35)-(4.39) with the slightly different adaptation

$$\beta^2 \to \lambda\ .$$

This gives the following result for $\lambda >> 2|\epsilon|$:

$$\overline{x(t)} = e^{-2t\lambda}\overline{x(0)}; \tag{4.62}$$

$$\overline{y(t)} = e^{-2t\lambda}\overline{y(0)}; \tag{4.63}$$

$$\overline{z(t)} = \overline{z(0)}, \tag{4.64}$$

so, as for white noise, we see a result that implies freezing.

4.8.2 Numerical results

For the numerical simulation of Poisson noise, we have solved the Schrödinger equation (4.47) numerically. This can be done in the following way:

1. Make a draw from a Poisson process with parameter λ as described in Remark 4.4.4. This gives us a set of clicks $\{t_1, t_2, \ldots, t_n\}$.
2. Solve the Schrödinger equation for the initial state $\psi(0)$ and the unperturbed Hamiltonian (2.2) numerically until $t = t_1$.
3. Multiply the state found in this way with U, i.e. $\psi(t_1) \to U\psi(t_1)$.
4. Continue to solve the Schrödinger equation for the unperturbed Hamiltonian numerically for the new initial state $\psi(t_1)$ at $t = t_1$ until $t = t_2$.
5. Multiply the state found in this way with U, i.e. $\psi(t_2) \to U\psi(t_2)$.
6. Continue in this way.

The figures below show our numerical results for $U \in \{\sigma_x, \sigma_y, \sigma_z\}$ with $\lambda = 0$, λ low and λ high each.

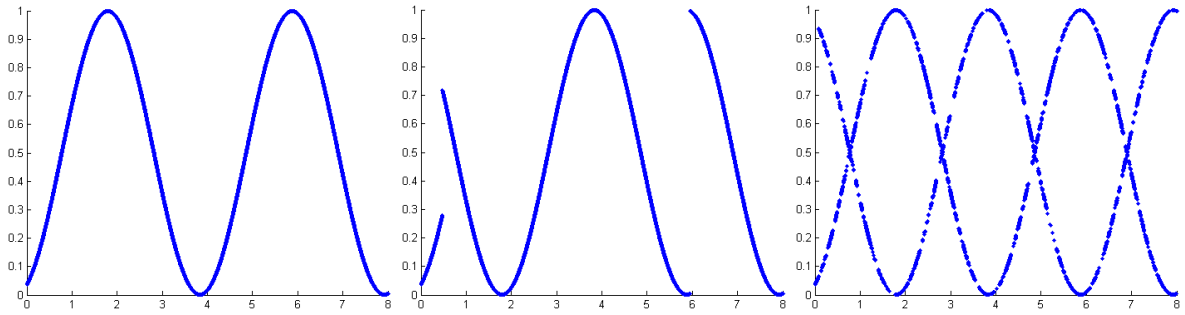

(a) $\lambda = 0$ (b) $\lambda = \lambda_b < \lambda_c$ (c) $\lambda = \lambda_c > \lambda_b$

Figure 4.7: Time evolution of the probability $P_L(t)$ for the two-level system with Schrödinger equation (4.47) for different λ and $U = \sigma_x$. The initial state is localized on the right. The first image has no noise, the second has moderate noise and the third has strong noise. In the middle image, it is easy to see the effect of a single jump caused by the noise. In the final image such jumps happen all the time, which makes it seem as if there are two functions in the graph. Localization clearly is not present, nor is a freezing effect.

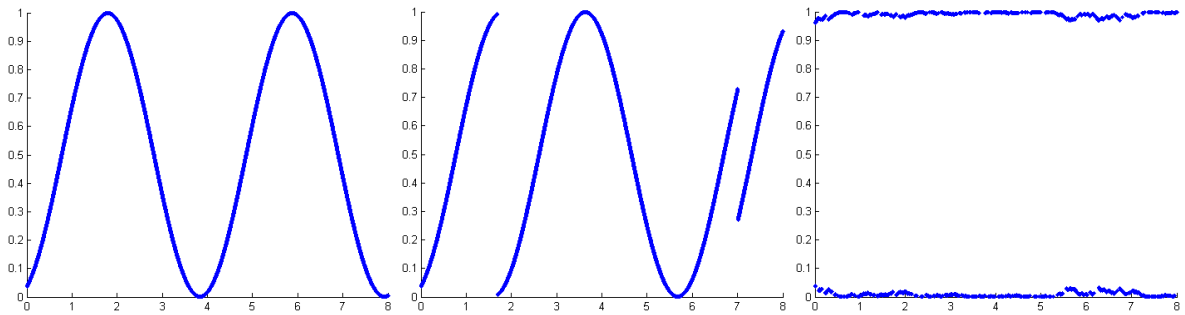

(a) $\lambda = 0$ (b) $\lambda = \lambda_b < \lambda_c$ (c) $\lambda = \lambda_c > \lambda_b$

Figure 4.8: Time evolution of the probability $P_L(t)$ for the two-level system with Schrödinger equation (4.47) for different λ and $U = \sigma_y$. The initial state is localized on the right. The first image has no noise, the second has moderate noise and the third has strong noise. In the middle image, it is easy to see the effect of a single jump caused by the noise. In the final image such jumps happen all the time, which makes it seem as if there are two functions in the graph. There is no localization.

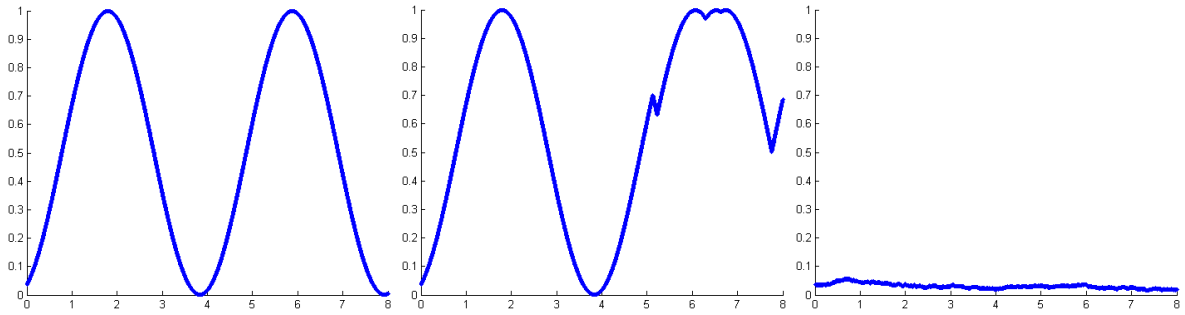

(a) $\lambda = 0$ (b) $\lambda = \lambda_b < \lambda_c$ (c) $\lambda = \lambda_c > \lambda_b$

Figure 4.9: Time evolution of the probability $P_L(t)$ for the two-level system with Schrödinger equation (4.47) for different λ and $U = \sigma_z$. The initial state is localized on the right. The first image has no noise, the second has moderate noise and the third has strong noise. For this choice of U, the system does not make a jump upon perturbation, but merely a 'bend'. For high λ, the state freezes to its initial position.

4.9 Localization

So far the results may have been a bit disappointing. They seem to implicate this cannot be a good model for Schrödinger's Cat, because there is no time-dependent localization. It turns out there is a set-up, however, that does give localization. We again use the Schrödinger equation (4.47) and study the time-evolution of the system numerically. However, we change $\hbar$ during the time evolution on the interval $[0, t_f]$. This is done by writing

$$\hbar(t) = f(t), \qquad \hbar(0) = \hbar_i, \qquad \hbar(t_f) = \hbar_f, \tag{4.65}$$

where f is some monotonicallly decreasing continuous function. The idea is that during a measurement, the classical description of the apparatus (as in the Copenhagen Interpretation) effectively makes $\hbar$ go to zero. Whether this true and how this works, is not something we will address here (it will be discussed in a bit more detail at the end of Chapter 5). To make sure the two-level system is a good model for the double well, we should also write $\epsilon(t)$ by using the energy splitting found in Chapter 3. In practise, this leads to the relation

$$\epsilon(t) = \hbar(t) \exp\left(\frac{1}{\hbar(t)}\right) . \tag{4.66}$$

Three possible outcomes of this set-up for linear f, $\psi(0) = (1, i)$, fixed λ and $U = \sigma_z$ can be seen in Figure 4.10.

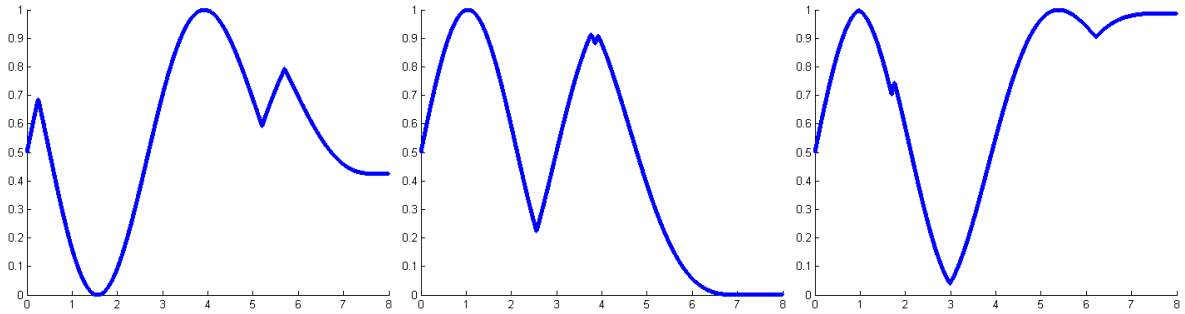

Figure 4.10: Three possible outcomes for the time evolution of the probability $P_L(t)$ in the two-level system with Schrödinger equation (4.47) for linear f, $\psi(0) = (1, i)$, fixed λ and $U = \sigma_z$. All three systems remain in their state after the final time of the image. The first does not localize, the second localizes to the right and the third localizes to the left.

It seems that this method may indeed lead to time-dependent localization, but definitely not in all cases. For a reasonable choice of f, it leads to localization in over half the cases. We will discuss the consequences of this at the end of Chapter 5. For now, it suffices to say this is a positive result.

Chapter 5

Double Well Potential

In this section, we finally look at the double well in a time-dependent way. As discussed in Chapter 1, we are interested in the behaviour of the (delocalized) ground state of the unperturbed potential in a perturbed potential. The main question is whether this delocalized state localizes in a time-dependent way due to these perturbations. This would provide a true solution to the problem of the double well potential, and it would provide more insight in the problem of Schrödinger's Cat. Because the time-dependent behaviour of the wave function in a perturbed double well is far from easy, most of our results have been obtained numerically.
The equation we have solved is the *time-dependent Schrödinger equation* for some time-dependent one-dimensional potential $V(t)$:

$$ih\frac{\partial\psi}{\partial t} = \frac{-\hbar^2}{2m}\frac{\partial^2\psi}{\partial x^2} + V(t)\psi, \tag{5.1}$$

where $\psi(0)$ is specified.

5.1 No perturbation

If the double well is to be an accurate model for Schrödinger's Cat, it should produce the collapse of the delocalized ground state to the left or to the right due to perturbations. With the use of the ground state ψ_0 and first excited state ψ_1, one can approximate the localized states. We therefore define

$$\psi_L \equiv \frac{1}{\sqrt{2}}(\psi_0 - \psi_1) \qquad\qquad \psi_R \equiv \frac{1}{\sqrt{2}}(\psi_0 + \psi_1), \tag{5.2}$$

where the index indicates whether the localization is left or right.
Before we look at the question whether a collapse to ψ_L or ψ_R takes place, we check what happens after such a collapse. Therefore, we now look at the following situation: due to a perturbation the wavefunction has (allegedly) collapsed to ψ_R. Afterwards, the potential is a normal double well potential. In this case we know that we can express the time evolution in terms of the eigenenergies of the problem:

$$\begin{aligned}\psi(t) &= \psi_0 e^{\frac{itE_0}{\hbar}} + \psi_1 e^{\frac{itE_1}{\hbar}} \\ &= e^{\frac{itE_0}{\hbar}}\left[\psi_0 + \psi_1 e^{\frac{it(E_1-E_0)}{\hbar}}\right].\end{aligned} \tag{5.3}$$

From the second expression, we see that the wave function oscillates from ψ_R to ψ_L with period

$$T = \frac{2\pi\hbar}{E_1(\hbar) - E_0(\hbar)}. \tag{5.4}$$

This effect would ruin the localization. We are interested, however, in the limit $\hbar \to 0$, which affects the period both directly (i.e. through the numerator) and indirectly through the energy splitting in the denominator. The calculations we have done in Chapter 3 tell us that

$$T = \frac{2\pi\hbar}{E_1(\hbar) - E_0(\hbar)} = 2\pi\frac{\sqrt{\pi e}}{\omega_0}\exp\left[\frac{1}{\hbar}\int_{-x_1}^{x_1}\sqrt{2m\left(V(x) - E_0^{(0)}\right)}dx\right]. \tag{5.5}$$

In this expression, ω_0 is the time a particle takes to move back and forth between the two turning points and this only depends on the shape of well. Since the exponential is always bigger than 1, the expression goes to infinity for $\hbar \to 0$. Therefore, the period of oscillation becomes exponentially large for small $\hbar$. We have also observed this numerically.

This conclusion has important implications. It means that localization, if it occurs, is not ruined by the oscillation between wells which is dictated by the Schrödinger equation. That, in turn, raises the question whether the wave function can become localized due to perturbations in the first place. We will try to answer that question in the next few sections.

5.2 Constant perturbation

In Section 3.2, we have seen that ψ_0 localizes in a time-independent way as $\hbar \to 0$ due to a single perturbation. In this section, we see if a single, constant perturbation can have this effect in a time-dependent way. Numerically, we have tested how ψ_0 evolves in a perturbed well for a number of single, constant perturbations and values of $\hbar$.

The symmetric double well potential we have used is the following:

$$V_0(x) = \frac{1}{750}\left[x^4 - 80x^2 + 1000\right]. \tag{5.6}$$

A perturbed version of this potential can be seen in Figure 5.1. The perturbation we have used is symmetric and C^∞ and can be specified by the location of its center b, its width $2c$ and its height d:

$$W_{b,c,d}(x) = \begin{cases} d\exp\left[\frac{1}{c^2} - \frac{1}{c^2-(x-b)^2}\right] & \text{if } |x-b| < c \\ 0 & \text{if } |x-b| > c \end{cases}. \tag{5.7}$$

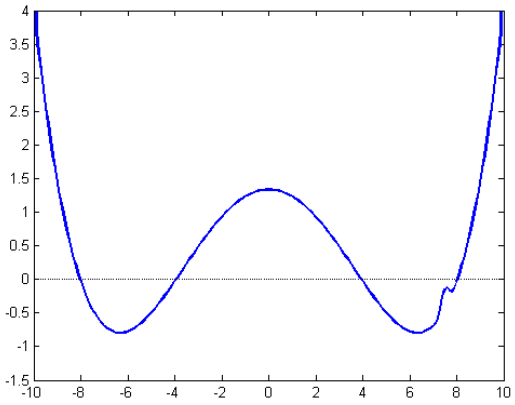

Figure 5.1: A double well potential (5.6) perturbed by (5.7) with $b = 7.5,\ c = 0.5,\ d = 0.3$ plotted for $x \in [-10, 10]$.

What kind of a result does this give when the initial state is ψ_0? That is easy to predict since the potential is time-independent. The result is an oscillation similar to (5.3):

$$\psi(t) = \left\langle \psi_0, \tilde{\psi}_0 \right\rangle \tilde{\psi}_0 e^{\frac{it\tilde{E}_0}{\hbar}} + \left\langle \psi_0, \tilde{\psi}_1 \right\rangle \tilde{\psi}_1 e^{\frac{it\tilde{E}_1}{\hbar}}, \tag{5.8}$$

where we denote the eigenstates and eigenenergies of the perturbed potential with a tilde. Of course, this oscillation means that no definitive localization takes place: after a while the system will always return to the initial state ψ_0. This behaviour can also be seen in the added movie *Constant Perturbation*.

5.3 Slowly rising perturbation

Here, we consider a perturbation (5.7) as before, but now it slowly rises for $t \in [0, T]$, i.e.

$$V(x,t) = \begin{cases} V_0(x) + W_{b,c,d}(x) \sin\left(\frac{\pi t}{2T}\right) & \text{if } t \leq T \\ V_0(x) + W_{b,c,d}(x) & \text{if } t > T \end{cases} . \tag{5.9}$$

It turns out that for some fixed $\hbar = \hbar_0$ and T, this actually gives time-dependent localization. An example can be seen in Figure 5.2 and the added movie *Rising perturbation 1*. This is not always the case, however. The behaviour not only depends on $\hbar$, but also on T, which is the time the perturbation takes to rise. Roughly one could say: when T is much bigger than the characteristic time $\hbar/E$ of a particle with energy E moving in the potential, the *adiabatic approximation* is applicable. This approximation is explained in [1, 23]. It implies that a particle in the original ground state ψ_0 slowly moves to the perturbed ground state $\tilde{\psi}_0$. By the results of Chapter 3, we know $\tilde{\psi}_0$ is localized (for $\hbar$ small enough). This would imply the occurrence of time-dependent localization, which is indeed what we observe for T big enough and $\hbar$ fixed. If however, T is small, this does not happen. If T is much smaller than $\hbar/E$, the *sudden approximation* is applicable (which is explained in [1]). That approximation says that nothing happens and the system simply remains in the delocalized state ψ_0. Indeed, this behaviour has been observed in our simulations as well.

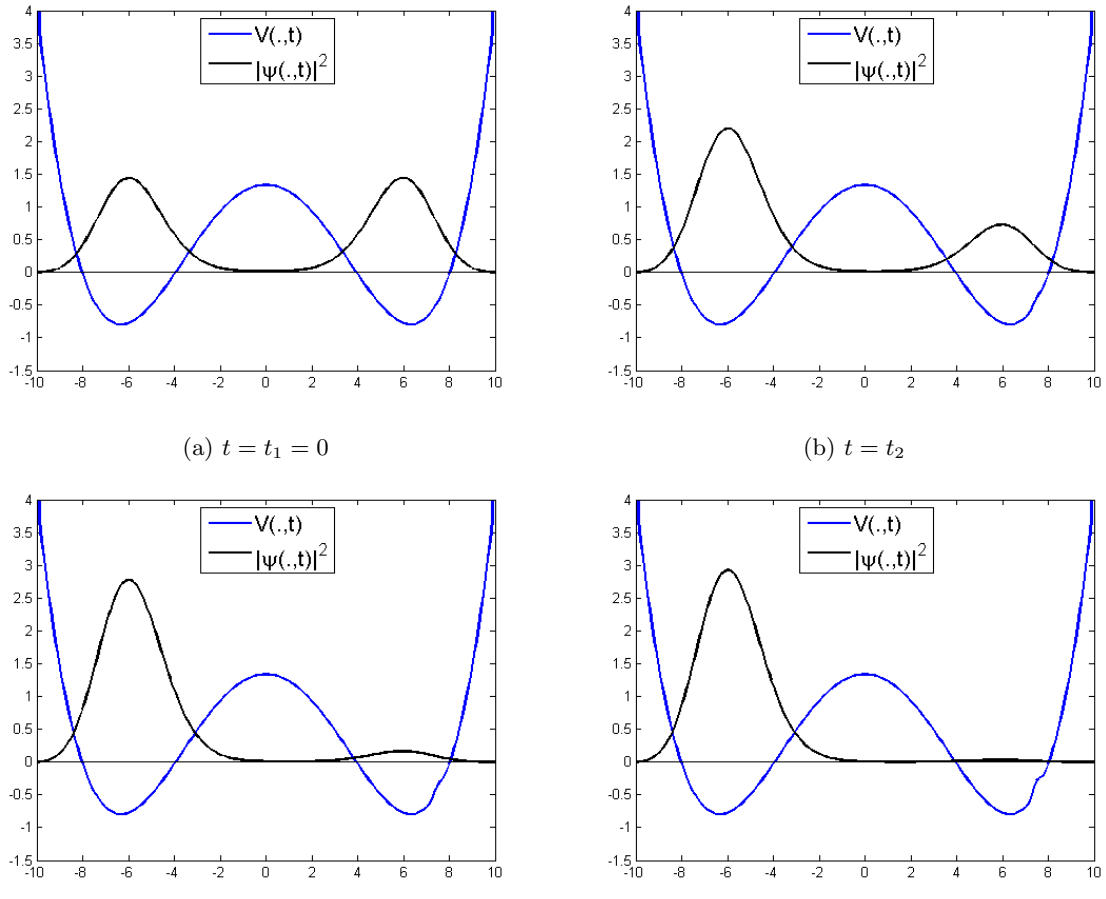

(a) $t = t_1 = 0$ (b) $t = t_2$

(c) $t = t_3$ (d) $t = t_4$

Figure 5.2: These images show the time dependent behaviour of $|\psi(.,t)|^2$ in the potential (5.9) for different t, where $0 = t_1 < t_2 < t_3 < t_4$. The initial state is the delocalized ground state ψ_0. The perturbation is quite small and slowly rises in the right well. The value of $\hbar = \hbar_0$ is fixed. After the perturbation has fully risen, the system keeps on oscillating a bit, but remains localized.

These conclusions for fixed $\hbar$ are important, but we are mostly interested in the classical limit. It turns out that no localization takes place in the limit $\hbar \to 0$, as can be seen in figure 5.3 and the added movie *Rising perturbation 2*. There, we consider the exact same situation for some $\hbar = \hbar_1 < \hbar_0$. The absence of localization can be understood: the wells effectively decouple in the limit $\hbar \to 0$, which causes the wave function to remain delocalized. A second explanation can perhaps be found in the approximations described above, because $\hbar$ and E change in the classical limit. However, further study of these approximation is required to confirm this.

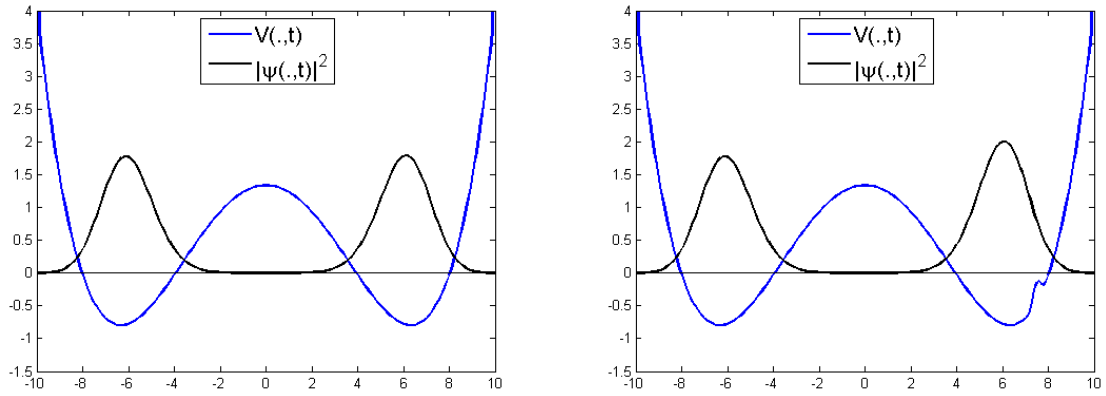

(a) $t = t_1 = 0$ (b) $t = t_2$

Figure 5.3: These images show the time dependent behaviour of $|\psi(.,t)|^2$ in the potential (5.9) for different t, where $0 = t_1 < t_2$. The initial state is the delocalized ground state ψ_0. The same perturbation as in Figure 5.2 slowly rises in the right well. The value of $\hbar = \hbar_1 < \hbar_0$ is fixed. No localization takes place due to the fact that tunneling is suppressed for small $\hbar$.

5.4 White Noise

We have simulated white noise processes in the way described in Remark 4.4.6 and added this noise to each point in space of the potential. This makes the potential look like the one in Figure 5.4, for example.

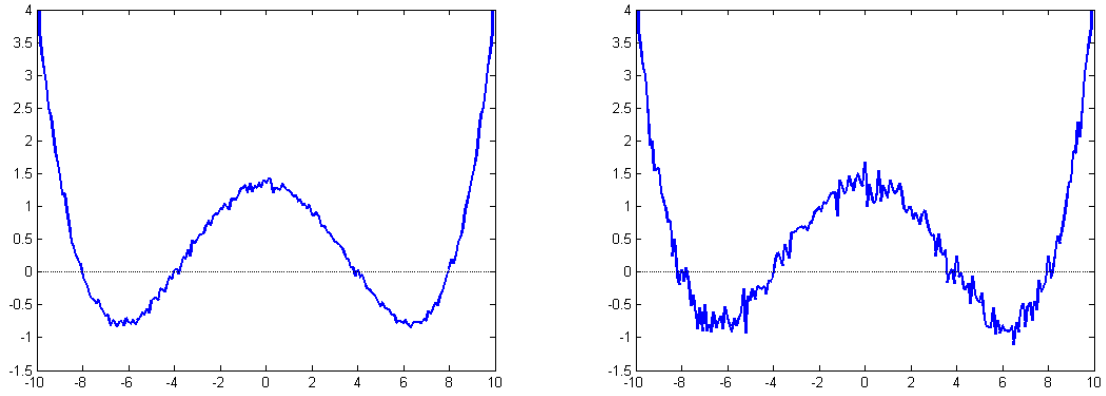

Figure 5.4: These two images show a double well potential disturbed by white noise of two variances at a certain point in time. The variance of the noise on the left is lower than the variance of the noise on the right.

To get an idea of the behaviour of the wave function in this potential, it is best to watch the added movies *White noise 1* (relatively high $\hbar$) and *White noise 2* (relatively low $\hbar$). It is difficult to capture this behaviour is a few images, so there are none added here. We will give a verbal description, however. For fixed $\hbar$, no localization takes place. It may happen temporarily, but never definitively, as can be seen in the movie *White noise 1*. This is in part due to the perturbations, but there is also a much simpler reason. As we have seen in Section 5.1, a localized wave function oscillates between the wells in an unperturbed potential. For fixed $\hbar$, this period is finite, and localization can therefore never be definitive. For $\hbar \to 0$, however, the period goes to infinity, so this oscillation would not bother us anymore. However, we then find the freezing effect also observed for the two-level system, as can be seen in the movie *White noise 2*. The oscillating behaviour does not bother us anymore, but localization does not happen either. This is hardly surprising: the wells effectively decouple, so perturbations barely have any influence on the localization. This is bad news if we want to use this as a model for Schrödinger's Cat.

5.5 Poisson Noise

To simulate Poisson noise, we have generated a Poisson proces as decribed in Remark 4.4.4. This gave us a set of times at which a perturbation in the form of (5.7) needed to appear. We then decided upon a size, width and height of the pertubation by making a random draw from a uniform distribution: $b \in [-10, 10], c \in [c_0/2, c_0], d \in [-d_0, d_0]$, where $c_0 > 0$, d_0 fixed. Finally, a similar draw was made for the time the perturbation lasted: $T \in [T_0/2, T_0]$ for some $T_0 > 0$. It was then added to the potential and taken away again with help of the sine function, quite similar to the first part of (5.9), but such that the perturbations disappeared in the same manner. Because of this method, multiple perturbations, smooth in both time and place, can be present at the same time. What the resulting potential looks like at any one time can be seen in Figure 5.5. Note that this Poisson noise is quite different from the one used in Chapter 4. There, the noise caused the state of the system to jump, whereas the noise has effect on the potential here. In both cases, however, the times at which the noise appears are generated by a Poisson process.

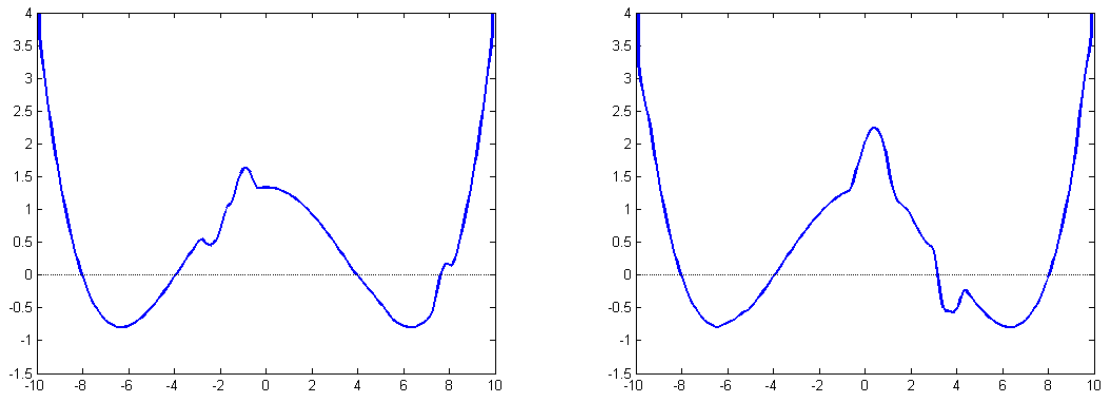

Figure 5.5: These two images show a double well potential disturbed by Poisson noise at two different times. In practise, a Poisson process generates clicks which are then turned into smooth perturbations in both time and space. The resulting potential could look like these two images.

Much as for white noise: for fixed $\hbar$, there may be temporary, but never definitive, localization. Because of the nature of the perturbations, Poisson noise does result in temporary localization more often than white noise. This behaviour can be seen in the added movie *Poisson noise 1*. As $\hbar \to 0$, the wave function freezes in its initial delocalized state, which can be seen in the movie *Poisson noise 2*.

5.6 Localization

For both white noise and Poisson noise we had two distinct cases. One the one hand, relatively large $\hbar$ resulted in time-dependent localization, but this was only temporary. On the other, relatively small $\hbar$ caused the wave function to remain in its original position, which meant that any present localization was preserved. If we could somehow combine these two cases, it would result in definitive time-dependent localization, which is required to describe Schrödinger's Cat. We therefore consider a system perturbed by Poisson noise, where $\hbar$ is not fixed. Numerically, this can be done by writing $\hbar(t)$ and letting $t \to \infty$. Motivated by the previous argument, we let $\hbar(t)$ decrease in time, so that the system slowly shifts from the first case to the second. This way, we hope to see time-dependent localization. For the two-level system this was sometimes the case, as has been discussed in Section 4.9.

It turns out this can indeed cause definitive time-dependent localization, as can be seen in the movie *Poisson with* $\hbar(t) \to 0$ - *localization*. For Schrödinger's Cat, this would mean the cat is either dead or alive, which is what we want to see. However, the movie *Poisson with* $\hbar(t) \to 0$ - *no localization* shows it might not lead to localization. In part, this depends on the shape of $\hbar(t)$. For reasonable dependence (e.g. linear), the wave function localizes in over fifty percent of the cases, depending on the particular realization of the underlying stochastic process. We have checked if there are certain choices for the dependence that result in localization almost every time, but that does not seem to be the case. One choice is definitely unwanted: if $\hbar(t)$ goes down really fast at the start, the wave function has no time to respond to the perturbations and it freezes right away.

To validate this model, the question whether and how $\hbar$ indeed effectively changes during a measurement should be answered. It will take much more research, however, to find an answer to that question. Nonetheless, the observation of this effect provides the first evidence that the problem of the classical limit of the double well, and hence that of Schrödinger's Cat, can be solved in this way.

Conclusion

It is time to summarize our findings and see if we can answer the questions posed at the beginning of this thesis. Subsequently, we look at what these answers might imply for Schrödinger's Cat and what should be looked at in further studies.

Time-independently, we saw that both the two-level system and the double well show localization due to a perturbation in the classical limit. Whether and how localization takes place, does not depend on the size of the perturbation, but rather on its location. However, the speed of localization (when taking the limit $\hbar \to 0$) does depend on the size of the perturbation. The numerical, mathematical and WKB conclusions about the wave function in a double well are all in agreement.

Time-dependently, we have found out quite a lot. For both the two-level system and the double well our conclusion can be stated as follows: a single perturbation can cause (temporary) localization, but in the limit $\hbar \to 0$ this effect disappears and the system remains in its initial state. Here, we mean that the experiment is repeated for different (but fixed) $\hbar$. Both systems, however, display time-dependent localization when $\hbar$ is allowed to decrease during the time evolution. This is not always the case, but it happens in at least fifty percent of all cases. This might be a hint that our model is a first step towards a solution of the problem. For Schrödingers's Cat, the localization means the cat is either dead or alive, rather than in a superposition of those states. However, in a good model for Schrödinger's Cat, this ought to happen in all cases. The double well as we studied it therefore cannot be a complete model of Schrödinger's Cat. There might be a way around this conclusion by assuming that localization does not always take place in reality. In that case, a measurement should be considered as failed when the wave function does not localize. Nonetheless, it seems safer to conclude that the model is incomplete.

In any case, some questions remain. The first question we should ask is whether and how $\hbar \to 0$ effectively happens during a measurement. The next one should be: is there a way we can adapt the model so that it produces time-dependent localization every time (i.e. with probability 1)? Perhaps this can done by adjusting the time scale of the noise and making use of the adiabatic approximation discussed in Section 5.3. It could also be that the double well cannot be adapted in this way: it might be too limited to be a complete model of Schrödinger's Cat. A model with more degrees a freedom, e.g. the quantum Ising model, could be more appropriate. Nonetheless, such a model would show some similarities with the double well, so part of our conclusions will remain valid.

Thus, more research is required to find out whether small perturbations can cause physical systems to leave their superposition in the classical limit, so that the problem of Schrödinger's Cat is avoided. Or, returning to the novelist's perspective once more: only time will tell whether our humble flea, a mere nuisance in everyday life, seizes power over life and death as soon as Schrödinger takes out his box.

Appendices

Appendix A

The WKB Approximation

In this appendix, we review the most important results of the semiclassical *Wentzel-Kramers-Brillouin (WKB) approximation*. This review is based on [1, 9]. Note that this is definitely not the most precise formulation of the WKB method available. A more rigorous treatment can be found in [6, 29], and a complete rigorous treatment in [10, 24]. The main results of this appendix are the WKB wave functions (A.15),(A.16) and the connection matrices (A.42),(A.43). These have been used in Section 3.1.

A particle of mass m obeys the Schrödinger equation

$$-\frac{\hbar^2}{2m}\frac{d^2\psi}{dx^2} = [E - V(x)]\,\psi, \tag{A.1}$$

which can be rewritten as

$$\frac{d^2\psi}{dx^2} = -\frac{p^2}{\hbar^2}\psi, \tag{A.2}$$

where

$$p(x) = \begin{cases} \sqrt{2m\,[E - V(x)]} & \text{if } E \geq V(x) \\ \pm i\sqrt{2m\,[V(x) - E]} & \text{if } E < V(x) \end{cases} . \tag{A.3}$$

For a particle with energy E in a potential $V(x)$ and $E > V(x)$ for every x, $p(x)$ is the classical expression for momentum. This analogy leads to the definition of the (generalized) de Broglie-wavelength

$$\lambda(x) = \frac{h}{p(x)} . \tag{A.4}$$

There are three cases: $E > V(x)$ (the classically allowed region without turning points), $E < V(x)$ (the classically forbidden region) and $E = V(x)$ (the turning points). The first two cases will now be treated separately.

A.1 The classically allowed region without turning points

For a constant potential $V = V_0$, the wave function in this region looks like

$$\psi(x) = Ae^{\pm\frac{i}{\hbar}\sqrt{2m[E-V_0]}x}. \tag{A.5}$$

Generally, the wave function again has this shape. However, it has a position dependent phase $S(x)$, so that

$$\psi(x) = Ae^{\frac{i}{\hbar}S(x)}. \tag{A.6}$$

Therefore, the Schrödinger equation (A.2) implicates that

$$-i\hbar S'' + (S')^2 = p^2. \tag{A.7}$$

We now expand $S(x)$ in terms of $\hbar$:

$$S(x) = S_0(x) + \hbar S_1(x) + \frac{\hbar^2}{2!} S_2(x) + \dots . \tag{A.8}$$

Plugging the wave function (A.6) into (A.7) and comparing terms with equal powers of $\hbar$ up to second order, we find three equations

$$\begin{aligned} &(S_0^{'})^2 = p^2, \\ &2S_0^{'}S_1^{'} - iS_0^{''} = 0 \ , \\ &S_0^{'}S_2^{'} + (S_1^{'})^2 - iS_1^{''} = 0 \ . \end{aligned} \tag{A.9}$$

The first equation can be solved right away:

$$S_0(x) = \pm \int^x p(y)dy, \tag{A.10}$$

where we do not give a lower bound for the integral since any constant can be aborbed in A. This allows us to solve the second equation

$$S_1(x) = \frac{i}{2} \log(p(x)) \ , \tag{A.11}$$

which in turn leads us to the solution of the third equation

$$S_2(x) = \mp \frac{p^{'}(x)}{2p^2(x)} \mp \int^x p(y) \left(\frac{p^{'}(y)}{2p^2(y)} \right)^2 dy. \tag{A.12}$$

The power series (A.8) can be stopped after two terms when $|\hbar S_2(x)/2 << 1|$, which can only hold if

$$\left| \frac{p^{'}(x)}{2p^2(x)} \right| << \frac{2}{\hbar}. \tag{A.13}$$

This is the case when the potential $V(x)$ changes very slowly as function of position. It also happens in the classical limit $\hbar \to 0$. Truncating the power series after two terms and filling in our solution for S_0 and S_1, we find

$$\frac{A}{\sqrt{p(x)}} e^{\pm \frac{i}{\hbar} \int^x p(y)dy} \ . \tag{A.14}$$

This is known as the WKB approximation of the wave function. The general solution under these (semiclassical) assumptions is

$$\boxed{\psi(x) \cong \frac{1}{\sqrt{p(x)}} \left[Ae^{\frac{i}{\hbar} \int^x p(y)dy} + Be^{-\frac{i}{\hbar} \int^x p(y)dy} \right].} \tag{A.15}$$

A.2 The classically forbidden region

Because $E < V(x)$ in this area, $p(x)$ is imaginary. Using a similar derivation as for the classical region (and replacing $p(x)$ with $\pm i\,|p(x)|$), the general solution under these assumptions can be found as

$$\boxed{\psi(x) \cong \frac{1}{\sqrt{|p(x)|}} \left[Ce^{-\frac{1}{\hbar} \int^x |p(y)|dy} + De^{\frac{1}{\hbar} \int^x |p(y)|dy} \right].} \tag{A.16}$$

A.3 Linear connection formulas

In order for the previous derivation to work, it is vital that the condition (A.13) holds. However, close to the classical turning points (where $E = V(x)$), we see that $p(x)$ becomes small. This means there is an area around the turning point where (A.13) does not hold. Therefore, the WKB approximation derived above is not applicable in this area. In this section, we derive formulas to connect the approximate wave function on the left and right side of these turning points. Before we start, we should remark there are two kinds of turning points. In figure A.1, x_1 is a *left-hand turning point* and x_2 is a *right-hand turning point*.

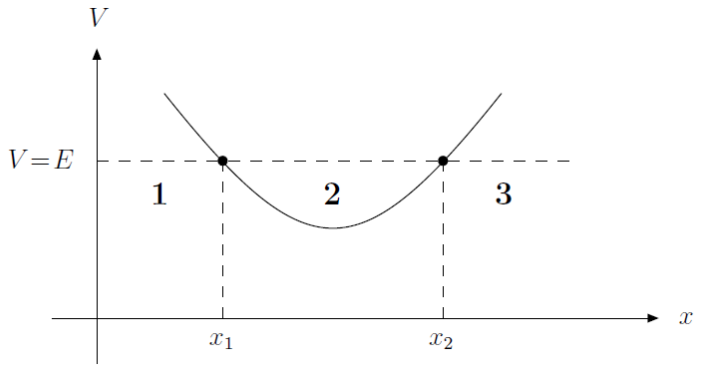

Figure A.1: A general potential well V. The particle has energy E. This provides us with turning points x_1 and x_2 and regions 1, 2 and 3. This picture has been taken from [1].

A.3.1 Airy functions

Airy functions are an important tool for finding the connection formulas. Suppose we have a linear potential with slope $V'(0)$ that has value E at the origin, i.e.,

$$V(x) = E + V'(0)x. \tag{A.17}$$

Putting this in the Schrödinger equation, we find

$$\frac{\hbar^2}{2m}\frac{d^2\psi}{dx^2} = V'(0)x\psi, \tag{A.18}$$

which can be rewritten as

$$\frac{d^2\psi}{dx^2} = \alpha^3 x\psi, \tag{A.19}$$

with

$$\alpha = \left[\frac{2m}{\hbar^2}V'(0)\right]^{1/3}. \tag{A.20}$$

We now define $z = \alpha x$ and change variables to find

$$\frac{d^2\psi}{dz^2} = z\psi\ . \tag{A.21}$$

This is where the two Airy functions $Ai(z)$ and $Bi(z)$ come in: they are the solutions to this equation. The Airy functions have an integral representation:

$$Ai(z) = \frac{1}{\pi}\int_0^\infty \cos\left(\frac{s^3}{3} + sz\right) ds, \tag{A.22}$$

$$Bi(z) = \frac{1}{\pi}\int_0^\infty \left[e^{-\frac{s^3}{3}+sz} + \sin\left(\frac{s^3}{3} + sz\right)\right] ds, \tag{A.23}$$

but for this derivation we use their asymptotic forms:

for $z >> 0$:

$$Ai(z) \approx \frac{1}{2\sqrt{\pi} z^{1/4}} e^{-\frac{2}{3}z^{3/2}} \tag{A.24}$$

$$Bi(z) \approx \frac{1}{\sqrt{\pi} z^{1/4}} e^{\frac{2}{3}z^{3/2}} \tag{A.25}$$

for $z << 0$:

$$Ai(z) \approx \frac{1}{\sqrt{\pi}(-z)^{1/4}} \sin\left[\frac{2}{3}(-z)^{3/2} + \frac{\pi}{4}\right] \tag{A.26}$$

$$Bi(z) \approx \frac{1}{\sqrt{\pi}(-z)^{1/4}} \cos\left[\frac{2}{3}(-z)^{3/2} + \frac{\pi}{4}\right] \tag{A.27}$$

A.3.2 Right-hand turning point

We now look at a right-hand turning point, conveniently placed at $x = 0$ (instead of the usual x_2). As can be seen in Figure A.1, $x < 0$ is classically allowed and $x > 0$ is classically forbidden. From (A.15) and (A.16), we know that the WKB approximation gives:

$$\psi(x) \cong \begin{cases} \frac{1}{\sqrt{p(x)}} \left[A e^{\frac{i}{\hbar}\int_0^x p(x')dx'} + B e^{-\frac{i}{\hbar}\int_0^x p(x')dx'} \right] & \text{if } x < 0 \\ \frac{1}{\sqrt{|p(x)|}} \left[C e^{-\frac{1}{\hbar}\int_0^x |p(x')|dx'} + D e^{\frac{1}{\hbar}\int_0^x |p(x')|dx'} \right] & \text{if } x > 0 \end{cases}. \tag{A.28}$$

We now assume the potential is linear in a small region around the turning point (called the *patching region*), as in (A.17). Therefore, the wave function is approximately a linear combination of Airy functions. We name this wave function the patching function ψ_{patch}:

$$\psi_{patch}(x) = aAi(\alpha x) + bBi(\alpha x). \tag{A.29}$$

Connecting for $x > 0$

We first connect the WKB solution for $x > 0$. We assume that we are far enough from the turning point for the Airy function to have the asymptotic behaviour in (A.24) and (A.25), but close enough for the linear approximation of the potential to be accurate. Here, the patching wave function takes the shape

$$\psi_{patch}(x) \cong \frac{a}{2\sqrt{\pi}(\alpha x)^{1/4}} e^{-\frac{2}{3}(\alpha x)^{3/2}} + \frac{b}{\sqrt{\pi}(\alpha x)^{1/4}} e^{\frac{2}{3}(\alpha x)^{3/2}}. \tag{A.30}$$

We now check at what the WKB wave function looks like for the linear approximation. With use of (A.17), it becomes clear that

$$p(x) = \sqrt{2m\left[E - V(x)\right]} = \sqrt{-2mV'(0)x} = \hbar\alpha^{3/2}\sqrt{-x}, \tag{A.31}$$

where α is defined as in (A.20). Therefore,

$$\int_0^x |p(x')|dx' \cong \hbar\alpha^{3/2} \int_0^x \sqrt{x'}dx' = \frac{2}{3}\hbar(\alpha x)^{3/2}. \tag{A.32}$$

So the WKB wave function becomes

$$\psi(x) \cong \frac{1}{\sqrt{\hbar}\alpha^{3/4}x^{1/4}} \left[C e^{-\frac{2}{3}(\alpha x)^{3/2}} + D e^{\frac{2}{3}(\alpha x)^{3/2}} \right]. \tag{A.33}$$

By comparing (A.30) with (A.33), we see that

$$a = \sqrt{\frac{4\pi}{\alpha\hbar}} C \qquad \text{and} \qquad b = \sqrt{\frac{\pi}{\alpha\hbar}} D. \tag{A.34}$$

Connecting for $x < 0$

Now we connect the WKB wave function to the patching wave function for $x < 0$. Again, we assume that we are far enough from the turning point for the Airy function to show the asymptotic behaviour in (A.26) and (A.27), but close enough for the linear approximation of the potential to be true. The patching wave function now looks like

$$\psi_{patch}(x) \cong \frac{1}{\sqrt{\pi}(-\alpha x)^{1/4}} \left[a \sin\left(\frac{2}{3}(-\alpha x)^{3/2} + \frac{\pi}{4}\right) + b \cos\left(\frac{2}{3}(-\alpha x)^{3/2} + \frac{\pi}{4}\right)\right], \tag{A.35}$$

which gives

$$\psi_{patch}(x) \cong \frac{1}{\sqrt{\pi}(-\alpha x)^{1/4}} \frac{1}{2} \left[(-ia + b) e^{i\pi/4} e^{i\frac{2}{3}(-\alpha x)^{3/2}} + (ai + b) e^{-i\pi/4}\, e^{-i\frac{2}{3}(-\alpha x)^{3/2}} \right]. \tag{A.36}$$

As for $x > 0$, we calculate

$$\int_0^x p(x')dx' \cong \hbar\alpha^{3/2} \int_0^x \sqrt{-x'}dx' = -\frac{2}{3}\hbar(-\alpha x)^{3/2}. \tag{A.37}$$

Therefore, the WKB wave function is

$$\psi(x) \cong \frac{1}{\sqrt{\hbar}\alpha^{3/4}(-x)^{1/4}} \left[A e^{-i\frac{2}{3}(-\alpha x)^{3/2}} + B e^{i\frac{2}{3}(-\alpha x)^{3/2}} \right]. \tag{A.38}$$

When we compare (A.36) with (A.38), we see that

$$A = \sqrt{\frac{\hbar\alpha}{4\pi}}(a - bi)e^{i\pi/4} \qquad \text{and} \qquad B = \sqrt{\frac{\hbar\alpha}{4\pi}}(-ai + b)e^{i\pi/4}\ . \tag{A.39}$$

By (A.34), this means

$$A = (Ci + \frac{1}{2}D)e^{i\pi/4} \qquad \text{and} \qquad B = (C - \frac{i}{2}D)e^{i\pi/4}\ . \tag{A.40}$$

When we shift the turning point back from 0 to x_2 and fill in our results, we find the WKB wave function around the right-hand turning point:

$$\psi(x) \cong \begin{cases} \frac{1}{\sqrt{p(x)}} \left[2C \cos\left(\frac{1}{\hbar}\int_{x_2}^x p(x')dx' + \frac{\pi}{4}\right) + D \sin\left(\frac{1}{\hbar}\int_{x_2}^x p(x')dx' + \frac{\pi}{4}\right)\right] & \text{if } x < x_2 \\ \frac{1}{\sqrt{|p(x)|}} \left[C e^{-\frac{1}{\hbar}\int_{x_2}^x |p(x')|dx'} + D e^{\frac{1}{\hbar}\int_{x_2}^x |p(x')|dx'} \right] & \text{if } x > x_2 \end{cases}. \tag{A.41}$$

A.3.3 The connection formulas in a matrix

Of course there also exist connection formulas for a left-hand turning point, which can be derived in a similar way. To distinguish between the two kinds of turning point we use the coefficients A_l, B_l, C_l and D_l for a left-hand turning point and A_r, B_r, C_r and D_r for a right-hand one. We use the coefficients like we do in (A.15) and (A.16). The lower limit of the integrals in these equations is always the coordinate of the turning point. These are the connection formulas for a left-hand turning point:

$$\begin{pmatrix} A_l \\ B_l \end{pmatrix} = \overbrace{e^{i\pi/4}\begin{pmatrix} \frac{1}{2} & -i \\ -\frac{i}{2} & 1 \end{pmatrix}}^{M_{C_l/D_l \to A_l/B_l}} \begin{pmatrix} C_l \\ D_l \end{pmatrix} \quad \text{or} \quad \begin{pmatrix} C_l \\ D_l \end{pmatrix} = \overbrace{e^{-i\pi/4}\begin{pmatrix} 1 & i \\ \frac{i}{2} & \frac{1}{2} \end{pmatrix}}^{M_{A_l/B_l \to C_l/D_l}} \begin{pmatrix} A_l \\ B_l \end{pmatrix}, \tag{A.42}$$

and for a right-hand turning point:

$$\begin{pmatrix} A_r \\ B_r \end{pmatrix} = \overbrace{e^{i\pi/4}\begin{pmatrix} 1 & -\frac{i}{2} \\ -i & \frac{1}{2} \end{pmatrix}}^{M_{C_r/D_r \to A_r/B_r}} \begin{pmatrix} C_r \\ D_r \end{pmatrix} \quad \text{or} \quad \begin{pmatrix} C_r \\ D_r \end{pmatrix} = \overbrace{e^{-i\pi/4}\begin{pmatrix} \frac{1}{2} & \frac{i}{2} \\ i & 1 \end{pmatrix}}^{M_{A_r/B_r \to C_r/D_r}} \begin{pmatrix} A_r \\ B_r \end{pmatrix}. \tag{A.43}$$

It turns out that these connection formulas actually have a one-directional nature, i.e. they can only be used one way. For an explanation of this fact and a more accurate derivation, we refer to [6, 29]. This one-directional nature is not really a problem for simple cases, which is why we discuss these connection formulas anyway.

Appendix B

Nondegeneracy of the ground state

In the proof of Proposition 3.2.6, we used the fact that the ground state of a certain Schrödinger operator is nondegenerate under certain assumptions. This resembles the Perron–Frobenius theorem in the finite-dimensional case, which we will first study. Then, we look at a proof of the nondegeneracy of the ground state. We follow the reasoning by both Glimm & Jaffe [8] and Reed & Simon [27, 28]. Finally, we check that the double well potential satisfies the pertinent conditions so that we may indeed use the nondegeneracy of the ground state.

B.1 Perron–Frobenius

The first version of the Perron–Frobenius theorem was proved by Perron in 1907 and dealt with matrices with strictly postive entries. In 1912, Frobenius extended it to matrices with non-negative entries, given an additional condition. The theorem is widely applicable as it stands, but, more importantly, it has a functional analytic analogue in which we are interested. To make this overview complete, we will first state the (relevant part of the) Perron-Frobenius theorem.

Definition B.1.1. An $n \times n$-matrix T over $\mathbb{R}$ is called

- *positive* if all the entries of T are positive (≥ 0).
- *strictly positive* if all the entries of T are strictly positive (> 0).
- *irreducible* if it is positive and $\forall\ 1 \leq i, j \leq n\ \ \exists\ k > 0$ such that $\left(T^k\right)_{ij} > 0$.

We will use the first two properties for general matrices (and vectors) as well.

Theorem B.1.2 (Perron–Frobenius)**.** *Let T be an irreducible matrix. Then T has a nondegenerate, strictly postive eigenvalue λ_0 such that $\forall\ \lambda$ eigenvalue of T: $|\lambda| \leq \lambda_0$.*
Furthermore, the eigenvector corresponding to λ_0 can be chosen to be strictly positive, and any other positive eigenvector is a multiple of this vector.

The first version of this theorem by Perron was a bit more limited. Instead of T be irreducible it demanded the matrix to be strictly postive. A proof of this theorem can be found in [34].

B.2 Nondegeneracy

From now on, we will continuously assume we are working in a Hilbert space $\mathcal{H}$ of the form $L^2(X, d\nu)$, where X is a measure space and $d\nu$ is a measure on X.

Definition B.2.1. A function $\psi \in \mathcal{H}$ is called

- *positive* if $\psi \geq 0$ almost everywhere (a.e.) and is not the zero function.
- *strictly positive* if $\psi > 0$ a.e.

Of course, these terms have negative analogues.
A bounded operator A on $\mathcal{H}$ is called

- *positive* if $\langle \psi, A\psi \rangle \geq 0 \ \forall \psi \in \mathcal{H}$. This is equivalent to $A = A^*$ and $\sigma(A) \subset \mathbb{R}^+$.
- *positivity preserving* if $A\psi$ is positive whenever ψ is positive.
- *positivity improving* if $A\psi$ is strictly positive whenever ψ is positive.
- *irreducible* if no non-trivial closed subspace of $\mathcal{H}$ is left invariant by both A and each bounded function $f \in L^\infty(X)$ (acting as a multiplication operator on $\mathcal{H}$). In other words: if $S \subset \mathcal{H}$ is a closed linear subspace of $\mathcal{H}$, and $\psi \in S$ implies both $A\psi \in S$ and $f\psi \in S$ for all $f \in L^\infty(X)$, then $S = \mathcal{H}$ or $S = \{0\}$.

Note that the final three properties for operators on $\mathcal{H}$ are analogues of the properties for matrices in Definition B.1.1. The theorem is also very similar, in the sense there exists a light version for strictly positive operators and a more general one for irreducible operators. We study the light one, as stated in [8], first.

Proposition B.2.2. *Let A be a bounded operator on $\mathcal{H}$. Suppose that A is positivity improving and that $\lambda = \|A\|$ is an eigenvalue of A.*
Then λ is a simple eigenvalue and the associated eigenvector ψ can be chosen to be strictly positive.

Proof. 1. First assume that ψ is real. We see that:

$$\lambda \|\psi\|^2 = \lambda \langle \psi, \psi \rangle = \langle \lambda\psi, \psi \rangle = \langle A\psi, \psi \rangle \leq \langle |A\psi|, |\psi| \rangle . \tag{B.1}$$

Since A is positivity preserving (improving, even), the fact that $|\psi| \pm \psi \geq 0$ implies that $A(|\psi| \pm \psi) \geq 0$. Therefore, we can conclude that $|A\psi| \leq A|\psi|$ and find that

$$\langle |A\psi|, |\psi| \rangle \leq \langle A|\psi|, |\psi| \rangle . \tag{B.2}$$

Moreover, by Cauchy–Schwartz:

$$\langle A|\psi|, |\psi| \rangle \leq \|A|\psi|\| \ \|\psi\| \leq \|A\| \ \|\psi\|^2 = \lambda \|\psi\|^2. \tag{B.3}$$

This means that (B.3) is an equality, which implies $A|\psi| = \lambda|\psi|$ (since the Cauchy–Schwartz inequality is an equality if and only if the arguments are linearly dependent), so $|\psi|$ is an eigenvector with eigenvalue λ. Of course, $|\psi|$ is positive, which means that

$$0 < \langle A|\psi|, \phi \rangle = \lambda \langle |\psi|, \phi \rangle , \tag{B.4}$$

since A is positivity improving. This has to be true for any ϕ, so $|\psi|$ needs to be strictly positive.

We now know that any real eigenvector ψ with eigenvalue λ is nonzero a.e., since $|\psi|$ is strictly positive. We have also shown that $|\psi|$ is an eigenvector with eigenvalue λ. These two facts leave us two options. The first is that $|\psi| - \psi$ is zero a.e., so ψ is strictly positive. The second is that $|\psi| - \psi$ is an eigenvector with eigenvalue λ, which means that $|\psi| - \psi$ is nonzero a.e., so ψ is strictly negative. Thus, each eigenvector with eigenvalue λ is either strictly positive or strictly negative. The existence of two independent eigenvectors with eigenvalue λ would therefore imply the existence of two strictly positive orthogonal vectors. By definition of the inner product on $\mathcal{H} = L^2(X, d\nu)$, that is impossible. Therefore, A has only one real eigenvector with eigenvalue λ.

2. Now assume that $\psi = \psi_0 + i\psi_1$, where ψ_0 and ψ_1 are both real (this is the general case). Since A is positivity preserving, it maps real functions to real functions. Therefore

$$A\psi = A\psi_0 + iA\psi_1 = \lambda\psi = \lambda\psi_0 + i\lambda\psi_1, \tag{B.5}$$

where $A\psi_0$ and $A\psi_1$ are both real. This implies that both ψ_0 and ψ_1 are eigenvectors of A with eigenvalue λ. By the first case, we conclude that ψ is a complex multiple of the unique real eigenvector, which completes the proof.

□

We now look at the more general theorem, as stated and proved in [28].

Proposition B.2.3. *Let A be a bounded, positive operator on $\mathcal{H}$. Suppose that A is positivity preserving and irreducible and that $\lambda = \|A\|$ is an eigenvalue of A.*
Then λ is a simple eigenvalue and the associated eigenvector ψ can be chosen to be strictly positive.

Proof. The proof of this statement is very similar to the one of Proposition B.2.2. Looking at that proof, we see that only one step uses the positivity improvingness of A (which is no longer supposed here), which needs to be replaced. It is the bit around (B.4), in which we conclude that $|\psi|$ is strictly positive. This is still true, bit it takes a bit more work to demonstrate. The rest of the proof remains valid and can be repeated.

Let $S = \{ f \in \mathcal{H} \mid f\psi = 0 \text{ a.e.}\}$, which is a closed subspace of $\mathcal{H}$. We first look at $S_+ = \{ f \in S \mid f \geq 0\}$. For $f \in S_+$, we see that

$$\langle Af, |\psi|\rangle = \langle f, A|\psi|\rangle = \lambda \langle f, |\psi|\rangle = 0, \tag{B.6}$$

where have used the fact that $A = A^*$ since A is positive. Since A is positivity preserving, Af is positive, and thus we can conclude from the above that $(Af)\psi = 0$ a.e., i.e. $Af \in S_+$. Now, we note that $S = S_+ - S_+ + i(S_+ - S_+)$, so that $f \in S$ implies $Af \in S$. Thus, S is left invariant by A. However, S is also left invariant by every function in $L^\infty(X)$ (because such functions act as a multiplication operators on $\mathcal{H}$). Because A is irreducible, we conclude that either $S = \mathcal{H}$ or $S = \{0\}$. The former is impossible, because $\psi \notin S$ since $\psi \neq 0$. Therefore, $S = \{0\}$, which implies that $|\psi|$ is strictly positive.

□

In [28], this proposition is applied to Schrödinger operators on $L^2(\mathbb{R}^\nu)$. It can be seen as the true 'nondegeneracy'-theorem.

Theorem B.2.4 (Nondegeneracy of the Ground State)**.** *Let $V \in L^2_{loc}(\mathbb{R}^\nu)$ be positive and suppose that $\lim_{|x|\to\infty} V(x) = \infty$. Then $-\Delta + V$ has a nondegenerate strictly positive ground state.*

Proposition B.2.3 is key in the proof of this theorem, which can be found in [28]. Nonetheless, it remains a difficult task to apply Proposition B.2.3 to Schrödinger operators and prove Theorem B.2.4. We will not give the full proof here, but merely a sketch:

1. Consider the operator $A = e^{-tH}$, where H is a positive operator which could be seen as the Hamiltonian (and should therefore be self-adjoint). Theorem B.2.4 deals with the special choice $H = -\Delta + V$ on $L^2(\mathbb{R}^\nu)$. We then check that this operator satisfies the conditions in Proposition B.2.3.

2. Positivity is not much of a problem since A is an exponential of a self-adjoint operator, which resembles the exponential of a real number.

3. The fact that A is positivity preserving follows from an expression of an integral kernel for e^{-tH}, which turns out to be the so-called *heat-kernel* if $V = 0$.

4. Irreducibility comes from the fact that H contains the Laplacian, hence the momentum operator. Together with position (whose bounded functions yield $L^\infty(\mathbb{R}^\nu)$), the momentum operator acts irreducibly on $L^2(\mathbb{R}^\nu)$.

A final, but very important remark: it is easy to check that the assumptions in Theorem B.2.4 hold for a potential V that satisfies the assumptions required for Theorem 3.2.2 and the additional demand that $\lim_{|x|\to\infty} V(x) = \infty$. Therefore, a general double well potential has a nondegenerate (strictly positive) ground state.

Appendix C

Numerical methods

A number of results in this thesis have been obtained with numerical methods. Here, we give a very brief theoretical overview of these methods. The discussion is based on [15]. For the actual implementation we have used Matlab.

We have used the so-called *implicit trapezoidal rule* to solve the one-dimensional Schrödinger equation numerically on the interval $[x_l, x_r] \times [0, t_f]$, where $t_f > 0$. That is, the equation we wish to solve is

$$\frac{\partial \Psi}{\partial t}(x,t) = \frac{-i}{\hbar} H(x,t)\Psi(x,t) = -\frac{i}{\hbar}\left[\frac{-\hbar^2}{2m}\left.\frac{\partial^2 \Psi}{\partial x^2}\right|_{(x,t)} + V(x,t)\Psi(x,t)\right] \equiv A(x,t,\Psi), \tag{C.1}$$

where we have introduced the function A, which gives the value of $\frac{\partial \Psi}{\partial t}(x,t)$ for given Ψ, x and t. To solve this equation, we suppose the solution is know at time $t = 0$.

Before we proceed, we need to know how A can be calculated from these values for fixed t. Let us fix t and suppose $\Psi(x,t) = \psi_t(x)$. If we know ψ_t in an analytical form, it is easy to determine $A(x,t,\Psi)$ with (C.1). However, because we are using numerical methods, we only have information about a finite set of points (say, $p+1$ in total, separated by a distance δ) in the interval $[x_l, x_r]$:

$$x_l = x_0 < x_1 < \ldots < x_{p-1} < x_p = x_r, \qquad x_{i+1} - x_i = \delta. \tag{C.2}$$

This means we only know $\psi_i \equiv \psi_t(x_i)$ for $0 \leq i \leq p$. In a similar fashion, we are only interested in A at a finite set of points: $A_i = A(x_i, t, \Psi)$. In order to determine the value of A at these points, we use the following approximation for a second order derivative, defined in terms of a new function $\tilde{A}$:

$$\left.\frac{\partial^2 \Psi}{\partial x^2}\right|_{(x_i,t)} = \left.\frac{\partial^2 \psi_t}{\partial x^2}\right|_{x_i} \approx \frac{\psi_{i+1} - 2\psi_i + \psi_{i-1}}{\delta^2} \ . \tag{C.3}$$

This approximation is simply a difference quotient, which can be derived by applying the common first order difference quotient twice. By putting this in (C.1), we obtain the following approximation for $A(x_i, t, \Psi)$:

$$A(x_i,t,\Psi) \approx \frac{-i}{\hbar}\left[\frac{-\hbar^2}{2m}\frac{\psi_{i+1} - 2\psi_i + \psi_{i-1}}{\delta^2} + V(x_i,t)\psi_i\right] \equiv \tilde{A}(x_i, t, \{\psi_i\}_{0\leq i\leq p}) \ . \tag{C.4}$$

In this equation it is actually true that $\psi_i = \Psi(x_i, t)$, but the approximation remains valid when $\psi_i \approx \Psi(x_i, t)$, which we will use in a moment.

Now that we can use $\tilde{A}$ to approximate A (and therefore $\frac{\partial \Psi}{\partial t}$) despite our limited information, it is time make things time-dependent. The first step is to divide the interval $[0, t_f]$ in m smaller ones of length ϵ:

$$0 = t_0 < t_1 < \ldots < t_{n-1} < t_m = t_f, \qquad t_{j+1} - t_j = \epsilon. \tag{C.5}$$

We would like to approximate the solution of (C.1) at the points $(x_i, t_j)_{0\leq i\leq p, 0\leq j\leq m}$. Therefore, we call our approximation of the solution at such a point $\psi_{(i,j)} \approx \Psi(x_i, t_j)$. From the known initial state (at $t_0 = 0$), we subsequently determine the state at the next point in time ($j \to j+1$) by solving the following equation for all $0 \leq i \leq p$:

$$\psi_{(i,j+1)} = \psi_{(i,j)} + \frac{1}{2}\epsilon\tilde{A}(x_i, t_j, \{\psi_{(k,j)}\}_{0\leq k\leq p}) + \frac{1}{2}\epsilon\tilde{A}(x_i, t_{j+1}, \{\psi_{(k,j+1)}\}_{0\leq k\leq p}), \tag{C.6}$$

where $\tilde{A}$ is defined as in (C.4). This equation makes sense if one considers the fact that A is defined as in (C.1), i.e. $\tilde{A}$ contains approximate information about $\frac{\partial\Psi}{\partial t}$. This method is known as the *implicit trapezoidal rule*. For j fixed, (C.6) is a set of p coupled equations that is not easy to solve. In Matlab it is simple, however, because it can be done by putting them in matrix form and using matrix division. That gives us the desired approximation of Ψ on $[x_l, x_r] \times [0, t_f]$. The method (C.6) can also be applied to the two-level system. In that case, the Hamiltonian does not contain a derivative, so $\tilde{A}$ takes a much simpler form.

One question remains: we have often used the ground state of some potential $V(x)$ as initial state in the application of the above method, but how can it be determined numerically? This can be done by writing the time-independent Schrödinger equation:

$$\frac{-\hbar^2}{2m}\left.\frac{d^2\psi}{dx^2}\right|_x + V(x)\psi(x) = E\psi(x). \tag{C.7}$$

Since we are working with a finite set of p points in space, this equation immediately leads to a set of p coupled equations through (C.3). Putting them in matrix form, it is clear that we are simply dealing with an eigenvalue problem, which can easily be solved by using the *Eig*-function in Matlab.

Of course, something should be said about the error which the used methods make. The implicit trapezoidal rule is reliable when dealing with the kinds of problems used in this thesis, as is explained in [15]. In this case, the error mainly depends on the size of δ and ϵ, which should be chosen smaller to get better results. We believe that they have been chosen small enough to get accurate results. For a real discussion on errors and methods which are more precise than the one used, we refer to [15] and books on numerical methods.

A final word on the numerical production of perturbations: Remark 4.4.4 describes how a Poisson process can be generated and Remark 4.4.6 does the same for white noise. Any perturbations can simply be added to $V(x, t)$ in (C.1), and the above method can be applied as usual.

Bibliography

[1] W. J. P. Beenakker. Dictaat bij het college Kwantummechanica 2. `http://www.hef.ru.nl/~beenakker/dictaat_QM2.pdf`, 2012. These lecture notes are in Dutch, but the front page contains a list of books on which it is based.

[2] P. Blanchard, G. Bolz, M. Cini, G. D. Angelis, and M. Serva. Localization stabilized by noise. *Journal of Statistical Physics*, 75:749–755, 1994.

[3] P. Busch, P. Lahti, and P. Mittelstaedt. *The Quantum Theory of Measurement*. Springer, 1996.

[4] P. Claverie and G. Jona-Lasinio. Instability of tunneling and the concept of molecular structure in quantum mechanics: the case of pyramidal molecules and the enantiomer problem. *Physical Review A*, 33:2245–2253, 1986.

[5] A. Einstein. Über die von der molekularkinetischen Theorie der Wärme geforderte Bewegung von in ruhenden Flüssigkeiten suspendierten Teilchen. *Annalen der Physik*, 322:549–560, 1905.

[6] N. Fröman and P. O. Fröman. *Physical problems solved by the phase-integral method*. Cambridge University Press, 2004.

[7] A. Garg. Tunnel splittings for one-dimensional potential wells revisited. *American Journal of Physics*, 68:430–437, 2000.

[8] J. Glimm and A. Jaffe. *Quantum physics*. Springer-Verlag, 1987.

[9] D. J. Griffiths. *Introduction to quantum mechanics*. Pearson, 1995.

[10] B. Helffer. *Semi-classical analysis for the Schrödinger operator and applications*, volume 1336 of *Lecture Notes in Mathematics*. Springer-Verlag, 1988.

[11] B. Helffer and J. Sjöstrand. Multiple wells in the semi-classical limit I. *Communications in Partial Differential Equations*, 9:337–408, 1984.

[12] C. Herring. Critique of the Heitler-London method of calculating spin couplings at large distances. *Reviews of Modern Physics*, 34:631–645, 1962.

[13] C. Herring and M. Flicker. Asymptotic exchange coupling of two hydrogen atoms. *Physical Review A*, 134:362–366, 1964.

[14] P. D. Hislop and I. M. Sigal. *Introduction to spectral theory*. Springer, 1996.

[15] W. Hundsdorfer. Lecture notes on Numerical Methods. `http://www.cwi.nl/~willem/Coll_NM11/NotesNM11.ps`, 2011. The second page contains a list of books on which it is based.

[16] G. Jona-Lasinio, F. Martinelli, and E. Scoppola. New approach to the semiclassical limit of quantum mechanics. *Communications in Mathematical Physics*, 80:223–254, 1981.

[17] G. Jona-Lasinio, F. Martinelli, and E. Scoppola. The semiclassical limit of quantum mechanics: a qualitative theory via stochastic mechanics. *Physics Reports*, 77:313–327, 1981.

[18] B. Kümmerer and H. Maassen. This book has yet to appear.

[19] B. Kümmerer and H. Maassen. The essentially commutative dilations of dynamical semigroups on M_n. *Communications in Mathematical Physics*, 109:1–22, 1987.

[20] L. D. Landau and E. M. Lifshitz. *Course of Theoretical Physics - 3. Quantum mechanics*. Pergamon Press, 1959.

[21] N. P. Landsman. Between Classical and Quantum. *Handbook of the Philosophy of Science*, Vol. 2: Philosophy of Physics:417–554, 2007.

[22] M. Maioli and A. Sacchetti. Two level system driven by a stochastic perturbation. *Journal of Statistical Physics*, 119:1383–1395, 2005.

[23] A. Mostafazadeh. The quantum adiabatic approximation and the geometric phase. *Physical Review A*, 55:1653–1664, 1997.

[24] D. Mouez and J. Sjöstrand. *Spectral asymptotics in the semi-classical limit*, volume 268 of *London Mathematical Society Lecture Note Series*. Cambridge University Press, 1999.

[25] B. Øksendal. *Stochastic Differential Equations: An Introduction with Applications*. Springer, 2010.

[26] A. N. Pechen. Quantum stochastic equation for a test particle interacting with a dilute Bose gas. *Journal of Mathematical Physics*, 45:400–417, 2004.

[27] M. Reed and B. Simon. *Methods of modern mathematical phyics - I. Functional analysis*. Academic Press, 1972.

[28] M. Reed and B. Simon. *Methods of modern mathematical phyics - IV. Analysis of operators*. Academic Press, 1978.

[29] K. Reijnders. Semiclassical theory of chiral tunneling in graphene. Master's thesis, Radboud University Nijmegen, 2011. Unfortunately, this thesis is not available on the Internet.

[30] E. Schrödinger. Die gegenwärtige Situation in der Quantenmechanik. *Naturwissenschaften*, 23:823–828, 1935.

[31] B. Simon. Semiclassical analysis of low lying eigenvalues II - Tunneling. *The Annals of Mathematics*, 120:89–118, 1984.

[32] B. Simon. Semiclassical analysis of low lying eigenvalues IV - the flea on the elephant. *Journal of Functional Analysis*, 63:123–136, 1985.

[33] D.-Y. Song. Tunneling and energy splitting in an asymmetric double-well potential. *Annals of Physics*, 323:2991–2999, 2008.

[34] A. Wassermann. Operators on Hilbert space. `http://iml.univ-mrs.fr/~wasserm/OHS.ps`, 1991.

[35] J. Wheeler and W. Zurek. *Quantum theory and measurement*. Princeton University Press, 1984.

A flea on Schrödinger's Cat

Supplement to thesis containing moving images

Robin Reuvers

August 2012

Classical Limit 1

Classical Limit 2

Oscillation

Constant perturbation

Rising perturbation 1

Rising perturbation 2

White noise 1

White noise 2

Poisson noise 1

Poisson noise 2

Poisson with $\hbar(t) \to 0$ - no localization

Poisson with $\hbar(t) \to 0$ - localization